Review

Not peer-reviewed version

Sesquiterpene Lactones as Promising Anti-Glioblastoma Drug Candidates Exerting Complex Effects on Glioblastoma Cell Viability and Proneural-Mesenchymal Transition

Andrey V. Markov *, Arseny D. Moralev, Kirill V. Odarenko

Posted Date: 16 December 2024

doi: 10.20944/preprints202412.1292.v1

Keywords: brain tumor; terpenes; tumor cell death; mitochondrial dysfunction; epithelial-mesenchymal transition; glial-mesenchymal transition; polypharmacology

 doi:10.20944/preprints202412.1292.v1

Review

Sesquiterpene Lactones as Promising Anti-Glioblastoma Drug Candidates Exerting Complex Effects on Glioblastoma Cell Viability and Proneural-Mesenchymal Transition

Andrey V. Markov *, Arseny D. Moralev and Kirill V. Odarenko

Institute of Chemical Biology and Fundamental Medicine, Siberian Branch of the Russian Academy of Sciences, Lavrent'ev Avenue 8, 630090 Novosibirsk, Russia

* Correspondence: andmrkv@gmail.com or markov_av@niboch.nsc.ru

Abstract: Glioblastoma is one of the most aggressive brain cancers, characterized by active infiltrative growth and high resistance to radiotherapy and chemotherapy. Sesquiterpene triterpenoids (STLs) and their semi-synthetic analogs are considered as a promising source of novel antitumor agents due to their low systemic toxicity and multi-target pharmacological effects on key processes associated with tumor progression. The current review aims to systematize the knowledge on the anti-glioblastoma potential of STLs accumulated over the last decade and to identify key processes in glioblastoma cells that are most susceptible to the action of STLs. Analysis of published data clearly demonstrated that STLs, which can successfully cross the blood-brain barrier, exert a complex inhibitory effect on glioblastoma cells through induction of the "mitochondrial dysfunction – oxidative stress – apoptosis" axis, inhibition of glucose metabolism and cell cycle phase transition, and suppression of glioblastoma cell motility and invasion through blockade of proneural-mesenchymal transition. Taken together, this review highlights the promising anti-glioblastoma potential of STLs, which are not only able to induce glioblastoma cell death, but also effectively affect their diffusive spread, and suggests possible directions for further investigation of STLs in the context of glioblastoma to better understand their mechanism of action.

Keywords: brain tumor; terpenes; tumor cell death; mitochondrial dysfunction; epithelial-mesenchymal transition; glial-mesenchymal transition; polypharmacology

1. Introduction

Glioblastoma multiforme (GBM) is one of the most aggressive forms of brain cancer, with an incidence ranging from 1 to 155 per 1,000,000 individuals in people younger than 20 years and older than 75 years, respectively [1]. Despite the fact that glioblastoma patients receive a full range of therapies, including deep tumor resection, tumor bed radiotherapy, and chemotherapy, the vast majority of these patients do not survive beyond 18 months [2], and their median progression-free survival (PFS) is only about 7 months from the time of diagnosis [3]. This alarming fact is directly related to the active diffuse spread of glioblastoma cells into healthy brain tissue, which makes it virtually impossible to completely remove tumor cells by maximal safe resection [4], and to the rapid acquisition of resistance to radiotherapy and chemotherapy by glioblastoma cells [5], which mediates a high probability of glioblastoma recurrence. Separately, it is necessary to note the extremely limited list of chemopreparations approved for glioblastoma therapy in the clinic, which is limited to alkylating agents, including temozolomide, and nitrosoureas, such as carmustine, lomustine, and fotemustine, and the anti-angiogenic humanized monoclonal antibody bevacizumab, the efficacy of which remains low, in part due to the high intertumoral heterogeneity of glioblastoma [6] and the ability of the tumor microenvironment to stimulate proneural-mesenchymal transition (PMT; also

 doi:10.20944/preprints202412.1292.v1

known as glial-mesenchymal transition), a process by which glioblastoma cells acquire a highly invasive mesenchymal phenotype that is resistant to therapeutic intervention [7].

Given the complex nature of glioblastoma pathogenesis with an extensive network of master regulators [8], in addition to the development of selective inhibitors of glioblastoma-related signaling proteins, the search for multitarget anti-glioblastoma drugs is of great interest and includes two main directions, namely drug repurposing (see recent comprehensive reviews [9,10]) and the synthesis of drug candidates based on multitarget natural metabolites [11]. In the latter case, among the wide variety of structural scaffolds used for the development of nature-based anti-glioblastoma agents, sesquiterpene lactones (STLs) deserve special attention due to their pronounced complex action against both tumor cells [12] and the tumor microenvironment [13–15], their ability to modulate a wide range of signaling pathways involved in glioblastoma pathogenesis, including PMT [12,16], and their ability to efficiently accumulate in brain tissues [17]. Despite the experimental data confirming the anti-glioblastoma potential of STLs, including their inhibitory effects on key glioblastoma-related processes, including glioblastoma cell motility and invasion [18–20], clonogenicity [21], expression of PMT marker proteins [22,23], and expansion of glioblastoma stem cells [24], there are still no comprehensive reviews summarizing, structuring, and analyzing this information. Only Yan et al. recently described the anti-glioma mechanisms of these compounds [19], but this review remains inaccessible to the broad scientific community because it is published only in Chinese. Some recent reviews provide brief information on the anti-glioblastoma activities of STLs, mainly describing their cell death inducing effects [20,25,26], which does not allow us to assess the prospects of this class of compounds as blockers of glioblastoma cell infiltration.

In this review, we summarize recent findings on the complex inhibitory effects of STLs, both natural and semisynthetic, on glioblastoma cells published in the last decade and answer the question of which processes in these cells are most susceptible to STLs. In addition, the pharmacological potential of STLs in relation to PMT was separately discussed.

2. Anti-Glioblastoma Activity of Sesquiterpene Lactones

2.1. Anti-Tumor Potency of STLs

Sesquiterpene lactones (STLs) are a broad class of secondary natural metabolites, mainly found in plants of the *Asteraceae* family, formed from three isoprene linkages and containing an α,β-unsturated α-methylene-γ-lactone ring, which allows STLs to react by Michael-type addition with biological nucleophiles (e.g, sulfhydryl groups of glutathione and cysteine residues), thereby determining their multi-target action on key processes associated with various pathologies, including malignant growth [27,28]. Based on the structure of the carbon skeleton, STLs can be classified into 7 major types, including germacranolides with a ten-membered ring, three types with a six-membered ring, namely elemanolides, eudesmanolides and eremophilanolides, and guaianolides, pseudoguaianolides and hypocretenolides with five- and seven-membered rings [14]. These compounds have promising complex anti-tumor effects against a wide range of tumors of different histogenesis, not only by causing tumor cell death through induction of apoptosis [25,26,29], necroptosis [30], ferroptosis [31], cytodestructive autophagy [32], and endoplasmic reticulum stress [33], but also by effectively blocking their capacity for high motility and invasion [34], spheroid growth [35], colony formation [36], adhesion to extracellular matrix [37], and vasculogenic mimicry [38], as well as by disrupting tumor cell energetics [39]. The pronounced anti-tumor potency of STLs has been demonstrated not only in vitro, but also in animal models, including murine xenograft models of non-small lung cancer [40], breast cancer [41], hepatocellular carcinoma [42], glioblastoma [18], neuroblastoma [33], and others. Currently, a number of STLs and their derivatives are undergoing clinical trials, including mipsagargin in patients with advanced solid tumors (phase I, completed) [43] and artesunate in patients with cervical intraepithelial neoplasia (phase I, completed) [44]. Thus, the accumulated material demonstrates the high antitumor potential of STLs and their ability to modulate various processes associated with tumor growth and metastasis.

 doi:10.20944/preprints202412.1292.v1

2.2. Criteria for Selection of Published Material and Structure of Analyzed Data

To perform a detailed analysis of the anti-glioblastoma activity of STLs, we used Google scholar and PubMed search engines to search for experimental articles published from 2014 to 2024 using the queries "sesquiterpene lactone" and "glioblastoma" or "glioma", followed by the selection of papers containing information on the direct pharmacological action of STLs on glioblastoma cells in vitro and in vivo. A total of 47 publications were identified that met the search criteria, describing the anti-glioblastoma activity of 28 natural and 5 semi-synthetic STLs belonging to the germacranolides (12 molecules), eudesmanes (2 molecules), guaianolides (12 molecules), edoperoxide-containing STLs (2 molecules), and STLs with other structural types (5 molecules) (Figure 1). A careful analysis of these reports revealed that the main attention of researchers has been focused on the analysis of STL-induced cell death, primarily their apoptogenic activity, while the effects of STLs on the processes associated with the infiltrative growth of glioblastoma, including PNMT, have been much less studied (Figure 2A). Because STLs generally have similar effects on the same characteristics of glioblastoma cells regardless of their structural affiliation (Table 1), in this review we have systematized the accumulated knowledge by focusing on STL-sensitive processes.

2.3. Direct Toxic Effect of PTLs on Glioblastoma Cells: Key Processes and Mechanisms

STLs were shown to be effective in suppressing glioblastoma cell viability in vitro, with cytotoxic effects mainly below 50 μM at 24-72 h incubation with a median IC_{50} (50% inhibitory concentration) of 16 μM (Table 1). Note that STLs inhibited the viability not only of various glioblastoma cells but also of patient-derived glioblastoma stem cells (GSCs), as shown for isocostunolide [45] and dimethylaminomicheliolide (DMAMCL) [24], demonstrating the high pharmacological potential of STLs against heterogeneous glioblastoma populations.

2.3.1. Pro-Apoptotic Effect of STLs in Glioblastoma Cells

Most of the reports analyzed indicate the apoptotic character of cell death under the action of STLs, including germacranolides (parthenolide [46], its derivatives parthenolide dimer [47], DMAPT-D6 [48] and 2 [49], isocostunolide [45], elephantopinolide A [50], costunolide [51], and molephantin [52]), guaianolides (micheliolide [53], DMAMCL [54–57], MCL3 [58], dehydrocostus lactone [18], brevilin A [59], xanthatin [60,61], lactucopicrin [22], tomentosin [62], cynaropicrin [63], and 9-oxomicheliolide [64]), eudesmane-type alantolactone [65,66], endoperoxide-containing dihydroartemisinin [67,68], and artesunate [69], as well as goyazensolide [70], deoxyelephantopin [71], and compounds 3 [72] and 4 [73]. The effect of these compounds on glioblastoma cells was accompanied by a number of apoptosis hallmarks, including phosphatidylserine externalization [45–50,52–54,58][59–64,67–69][71–73], cleavage of poly(ADP-ribose) polymerase 1 (PARP-1) [22,48,52,59,61,65,66,68], and activation of executioner caspases, among which activation of caspase-3 was predominantly observed [45–50,52–54,58][59–64,67–69][71–73]; only elephantopinolide A and molephantin were found to activate caspase-7 [50,52], and lactucopicrin cleaved pro-caspase-6 [22]. Activation of caspase-3/-7 was preceded by cleavage of pro-caspase-9 in most published reports (Table 1), suggesting that the mitochondrial pathway of apoptosis is triggered by STLs.

 doi:10.20944/preprints202412.1292.v1

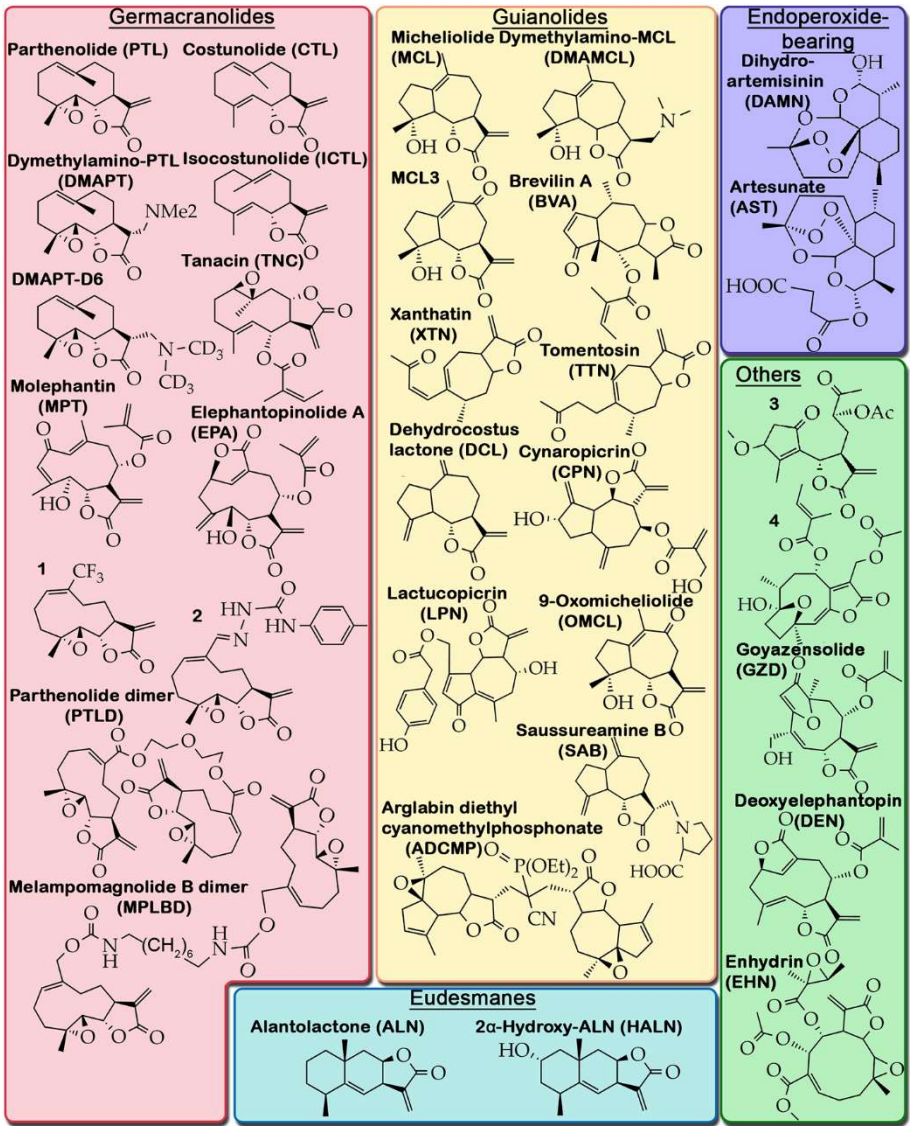

Figure 1. Structures of natural STLs and their derivatives with anti-glioblastoma activities.

These data are consistent with the ability of STLs to modulate the expression of Bcl-2 family proteins that control mitochondrial membrane permeability in glioblastoma cells [74], including increasing the Bax/Bcl-2 ratio [18,47,51–54,60,65,71], downregulating Mcl-1 [58,73], and upregulating Bak [59]. These perturbations resulted in massive loss of mitochondrial membrane potential [50,52,59,63,68,72] and release of cytochrome C from mitochondria into the cytosol [18,53,59,63,65,66,71]. Interestingly, on the background of inducing mitochondrial apoptosis in glioblastoma cells, costunolide and tomentosine also effectively activated caspase-8 [51], and DMAPT-D6 significantly activated the expression of death receptors DR3 and DR5 and adapter proteins FADD and TRADD [48,62], suggesting the ability of STLs to induce glioblastoma cell death also by intrinsic receptor-dependent apoptosis, although this effect of STLs is still poorly understood. In addition to activating the caspase cascade, STLs stimulated the expression of p53, a key apoptosis-related regulator whose suppressed function promotes glioblastoma progression [75]. Pronounced p53-inducing activity in glioblastoma cells has been shown for costunolide [51], DMAPT-D6 [48], lactucopicrin [22], and dihydroartemisinin [76], the latter also increasing the phosphorylation level of p53 [76], a necessary step for the realization of p53-mediated transcriptional programs [77].

Preprints.org (www.preprints.org) | NOT PEER-REVIEWED | Posted: 16 December 2024 doi:10.20944/preprints202412.1292.v1

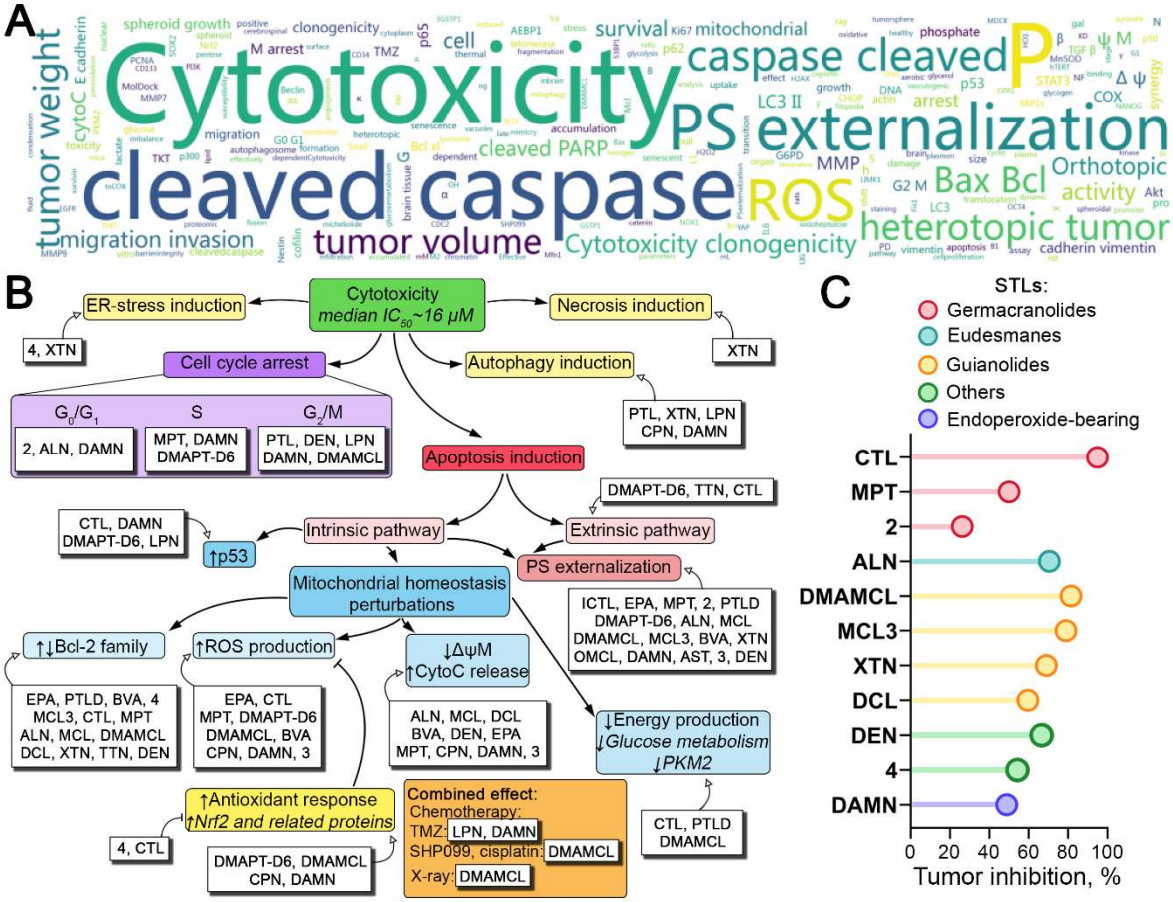

Figure 2. Anti-glioblastoma effects of natural STLs and their derivatives. (A) Word cloud plot of keywords obtained from anti-glioblastoma activities of STLs summarized from Table 1. (B) Effect of STLs on key processes associated with glioblastoma cell death. Downward (↓) and upward (↑) bold arrows indicate downregulation and upregulation of the processes, respectively. Dull arrows (⊥) indicate inhibition. (C) In vivo anti-glioblastoma effects of STLs in subcutaneous xenograft models. Different colors represent different types of STLs.

2.3.2. Pro-Oxidant Effect of STLs in Glioblastoma Cells

The above data suggest a pronounced mitochondria-targeting effect of STLs underlying their potent anti-glioblastoma potency. More detailed studies revealed that STLs not only disrupted the homeostasis of Bcl-2 family proteins, but also affected processes controlling mitochondrial dynamics in glioblastoma cells. Alantolactone was found to cause dephosphorylation of cofilin with its subsequent translocation to mitochondria together with G-actin in U87 cells [66]. Given the key regulatory function of cofilin in actin assembly, which plays an important role in mitochondrial fission, mitochondrial shape changes and mitophagy [78], this translocation induced cofilin-actin pathology leading to mitochondrial dysfunction [79], accompanied by cytochrome C release [80]. Molephantin was also found to modulate the levels of proteins that control mitochondrial dynamics, inhibiting the expression of Mfn1/2 and OPA1 and upregulating Fis1 and Drp1, leading to mitochondrial fragmentation and massive mitochondrial depolarization in glioblastoma cells [52].

 doi:10.20944/preprints202412.1292.v1

Table 1. Anti-glioblastoma activity of STLs.

Type	Compound	Cell line	Concentration	Biological effects	Effects on cell signaling	Ref.
Germacranolides	Parthenolide (PTL)	U373	8–16 μM	Cytotoxicity ($IC_{50}^{(24\ h)}$ ~ 17 μM); ↓survivin, G_2/M arrest, ↑phosphatydilserine (PS) externalization, ↑cleaved caspase-3, ↑cytoplasm vacuoles, ↑LC3-II/LC3-I	↓Cdk2, ↑Chk2, ↑ULK1	[46]
	Dimethylaminoparthenolide (DMAPT)	9LSF	5–25 μM 40 mg/kg, i.p.[1]	In vitro: Cytotoxicity ($IC_{50}^{(48\ h)}$ ~ 7 μM) In vivo (BBB permeability): Effective uptake by orthotopic 9LSF tumor in rats	ND[2]	[81]
		U87, GBM6, GL261	1–10 μM; 100 mg/kg (30 times)	In vitro: Cytotoxicity (IC_{50} = 3.5–8.8 μM) In vivo (BBB permeability): accumulation in brain of healthy mice (6251 ng/g (1 h); brain-to-plasma ratio: 2.1 (1 h) and 3.0 (4 h)) In vivo (GL261; orthotopic): ↑survival	ND	[82]
	Tanacin (TNC)	U87	1–20 μg/mL	Cytotoxicity ($IC_{50}^{(48\ h)}$ = 4.5 μg/mL)	ND	[83]
	Isocostunolide (ICTL)	Glioma stem cell lines: GSC-3#, GSC-12#, GSC-18#	0.1–10 μg/mL	Cytotoxicity ($IC_{50}^{(72\ h)}$ = 1.1–2.8 μg/mL), ↑PS externalization, ↑cleaved caspase-3, ↓spheroidal growth, ↓colony formation capacity	ND	[45]
	Elephantopinolide A (EPA)	U87	1–50 μM	Cytotoxicity ($IC_{50}^{(48\ h)}$ = 4.22±0.11 μM), ●[3]GSTP1 (molecular docking (MolDock), thermal shift assay), ↓GSTP1, ↑PS externalization, ↑chromatin condensation, apoptosis (Acridine orange/ethidium bromide staining), ↑cleaved caspase-7, ↑Bax, ↓Bcl-xl, $\downarrow\Delta\psi_M$[4], oxidative stress: ↑mitochondrial ROS, ↑H_2O_2, ↑·OH, ↑lipid peroxidation	↓JNK1 (mRNA, protein), ↑p-JNK, ↑p-STAT3	[50]
	Costunolide (CTL)	A173, U87	10–40 μM 5 mg/kg, i.p. (10 times)	In vitro: ROS-dependent cytotoxicity ($IC_{50}^{(24\ h)}$ ~ 30 μM), ↑ROS, ↓telomerase activity, ↓hTERT, ↑p53, ↑caspase-3/8 activity, ↑Bax/Bcl-2, ↓glucose metabolism: ↓G6PD, ↓TKT, ↓TKT activity; ↑senescence: ↑β-gal-cell staining, ↑GS(P), ↑glycogen accumulation	↓Nrf2	[51]

 doi:10.20944/preprints202412.1292.v1

Type	Compound	Cell line	Concentration	Biological effects	Effects on cell signaling	Ref.
				In vivo (U87, heterotopic): ↓tumor volume, ↓tumor weight, ↓telomerase activity, ↑ROS, ↑caspase-3/8 activity, ↓TERT, ↓G6PD, ↓TKT, ↓GS(P)		
	Molephantin (MPT)	U251, U87	3–100 μM 10 and 30 mg/kg, i.p. (10 times)	In vitro: Cytotoxicity ($IC_{50}^{(72\ h)}$ = 10.6–22.6 μM), ↓colony forming capacity, S arrest, ↓migration, ↓invasion, ↓vimentin, ↓Snail, ↓N-cadherin, ↑E-cadherin, ↑PS externalization, ↑Bax/Bcl-2, ↑ROS, ↑cleaved caspase-7/9/3, ↑cleaved PARP, ↑mitochondrial ROS, ↓$\Delta\psi_M$, ↑mitochondrial dynamic imbalance (↓Mfn1/2, ↓OPA1, ↑Fis1, ↑Drp1, ↑mitochondrial fragmentation), ↓late stage mitophagy, ↓autophagosome-lysosome fusion, ↓spheroid growth In vivo (U87, heterotopic): brain tissue accumulation, ↓tumor volume, ↓tumor weight, no organ toxicity, ↑Bax/Bcl-2, ↑cleaved caspase-9/7/3, ↑cleaved PARP	↓CDK4, ↓CDK2, ↑p21, ↓p-PI3K, ↓p-Akt, ↓p-mTOR,	[52]
	Melampomagnolide B dimer (MPLBD)	9L-SF	3–10 μM	Cytotoxicity	ND	[84]
	1 (смотри 32)	C6	ND	IC_{50} = 3.0±0.8 μM	ND	[85]
	2 (4d)	U87, MC38	1–16 μM 40 mg/kg, p.o.[5] (12 times)	In vitro: Cytotoxicity ($IC_{50}^{(96\ h)}$ = 2.8 μM), ↑PS externalization, G_0/G_1 arrest In vivo (MC38, heterotopic): ↓tumor weight, no organ toxicity	●NF-κB (MolDock)	[49]
	Parthenolide dimer (смотри 5) (PTLD)	U87, U118, SF126, SHG44, U251, C6	1–10 μM 50 mg/kg, i.p. (6 times)	In vitro: Cytotoxicity ($IC_{50}^{(72\ h)}$ = 1.66–7.93 μM), ↓clonogenicity, ↑PS externalization, ↓migration, ↓invasion, ●PKM2 (molecular docking, thermal shift assay), ↑E-cadherin, ↓vimentin, ↑Bax/Bcl-2, ↓Bcl-xl In vivo (U118, heterotopic): ↓tumor volume, ↓tumor weight, ↑Bax/Bcl-2, ↑E-cadherin, ↓vimentin, ↓STAT3 MDCK cells: ↓barrier integrity	↓STAT3, ↓p-STAT3, ↑PDK4	[47]
	DMAPT-D6	U87, LN229	2.5–40 μM	ROS-dependent cytotoxicity (IC_{50} = 11.15–15.5 μM), ↓clonogenicity, S arrest, ↑ROS, ↑DNA damage (↑γH2AX, ↑p53, ↑53BP1, ↑LIG IV), ↑PS externalization, ↑cleaved caspase-3, ↑cleaved PARP	↓cyclin B, ↓cyclin E, ↓CDK1, ↓CDK2, ↑p27, ↑Nrf2, ↑DR3, ↑DR5, ↑FADD, ↑TRADD	[48]

 doi:10.20944/preprints202412.1292.v1

Type	Compound	Cell line	Concentration	Biological effects	Effects on cell signaling	Ref.
Eudesmanes	Alantolactone (ALN)	U87, U251, U118	1–50 μM 10 and 20 mg/kg, i.p. (15 times)	In vitro: Cytotoxicity ($IC_{50}^{(48\ h)}$ = 16.33–29.16 μM), ↓clonogenicity, G_0/G_1 arrest, ↓migration, ↓invasion, ↓MMP-2, ↓MMP-9, ↑PS externalization, ↑cleaved caspase-3/9, ↑cleaved PARP, ↑Bax/Bcl-2, ↑cytoplasmic cytochrome C (cytoC), ↓COX-2 In vivo (U87, heterotopic): ↓tumor weight, ↓tumor volume, ↓COX-2, ↓p-p65 In vivo (BBB penetration): present in cerebrospinal fluid	↓Cyclin D1, ↓CDK4, ↓binding of NF-κB p50/p65 and p300 to COX-2 promoter, ↓nuclear translocation of p65/p50, ↓p-IκB-α, ↓p-IKKβ, ↓IKKβ kinase activity, ●IKKβ (MolDock)	[65]
		U87, U251	10 μM 20 mg/kg, i.p (15 times)	In vitro: ↑G-actin, ↓F-actin, ↑mitochondrial transition of F-actin, ↓p-cofilin, ↑mitochondrial transition of cofilin, ↓migration, ↓invasion, ↓MMP-2, ↓MMP-9, ↑PS externalization, ↑cleaved caspase-3/9, ↑cleaved PARP, ↑cytoC In vivo (U87, heterotopic): ↓p-cofilin, ↓p-LIMK1/2	↓p-LIMK1/2	[66]
		HCM3, U87, U251	10–50 μM 20 mg/kg, i.p. (7 times)	In vitro: Cytotoxicity (IC_{50} = 10–30 μM), ↓spheroid growth, ↓CD133, ↓OCT4, ↓SOX2, ↓NANOG In vivo (U87, orthotopic): ↑survival, ↓tumor size, ↓p-EGFR, ↓p-YAP	↓YAP, ↑p-YAP, ↓p-EGFR, ↑p-LATS1	[86]
	2α-Hydroxyalantolactone (HALN)	U87, U87ΔEGFR	0.1–100 μM	Cytotoxicity (IC_{50} = 15.15–49.22 μM)	ND	[87]
Guaianolides	Micheliolide (MCL)	U251	2.5–20 μM	Cytotoxicity ($IC_{50}^{(48\ h)}$ = 12.5±1.6 μM), ↓filopodia formation, ↓clonogenicity, ↓migration, ↓invasion, ↓MMP-9, ↓N-cadherin, ↓vimentin, ↑PS externalization, ↑cytoC, ↑cleaved caspase-3/9, ↑Bax/Bcl-2, ↓COX-2	↓p-IκBα/ IκBα	[53]
	Dimethylaminomicheliolide (DMAMCL, ACT001)	C6, U87	1–120 μM 25–100 mg/kg, p.o. (21 times)	In vitro: Cytotoxicity ($IC_{50}^{(72\ h)}$ = 20.58–27.18 μM), ↑PS externalization, ↑Bax/Bcl-2 In vivo (C6, orthotopic): ↓tumor weight, ↑survival, no organ and brain toxicity In vivo (BBB permeability): effectively accumulated in brain tissue (19.0±9.6 μg/mL (0.5 h))	ND	[54]
		U118, U251, U87,	5–40 μM	Cytotoxicity ($IC_{50}^{(48\ h)}$ = 17.9–37.1 μM), ↓clonogenicity, ●PKM2 (micheliolide (DMAMCL metabolite), pull-	ND	[21]

 doi:10.20944/preprints202412.1292.v1

Type	Compound	Cell line	Concentration	Biological effects	Effects on cell signaling	Ref.
		SF126, SHG44		down), ↑pyruvate kinase activity, ↓aerobic glycolysis and ↓pentose phosphate pathway (↓lactate, ↓glucose-6-phosphate, ↓sedoheptulose-7-phosphate, ↓glycerol-3-phosphate)		
		GL261	0.2–100 μM 50 mg/kg, p.o. + 2 Gy X-ray (5 times)	In vitro: ↑susceptibility of GL261 cells to X-ray, ↑ROS, ↑DNA damage, ↑cleaved caspase-3 In vivo (GL261, heterotopic): ↓tumor volume (+X-ray)	ND	[55]
		U87	10 μM 200 mg/kg, p.o. (6 times)	In vitro: ●PAI-1 (proteomic analysis, thermal shift assay, pull-down, surface plasmon resonance (K_D = 2.31 mM), MolDock), ↓migration, ↓invasion, ↓vasculogenic mimicry, ↑PS externalization, synergy with cisplatin, ↑E-cadherin, ↓vimentin, ↓Snail, ↓β-catenin In vivo (U118, heterotopic): ↓tumor size, ↓tumor weight, ↓p-PI3K, ↓p-Akt	↓p-PI3K, ↓p-Akt	[56]
		U251, TJ905	20–80 μM 400 mg/kg/day, p.o.	In vitro: ↓PD-L1 In vivo (GL261, orthotopic): ↑survival, ↓PD-L1, ↓p-STAT3, ↓M2 macrophage infiltration	↓p-STAT3, ●STAT3 (pull-down)	[15]
		U118, U251, SF126, SHG44, GL261	0.1–100 μM 200 and 400 mg/kg/day, p.o.	In vitro: Cytotoxicity (IC_{50} = 7.3–77.3 μM), G_2/M arrest, ↑PS externalization. ↑ROS, ↑NOX1, ↑TrX, ↑HO1, ↓MnSOD In vivo (U118, heterotopic): ↓tumor weight, ↓tumor volume In vivo (GL261, orthotopic): ↓tumor volume, ↓CDC2, ↓cyclin B1, ↓p-p65, ↓MnSOD, ↓Ki67	●IKKβ (pull-down, LC-MS/MS), ↓IKKγ, ↓p-IKKβ, ↓p-IκBα, ↓p-p65, ↓p-p65 nuclear translocation, ↓β-TRCP, ↑Nrf2	[57]
		patient-derived GSC 1123, R39	1–100 μM 100 mg/kg, p.o. (5 times)	In vitro: Cytotoxicity (IC_{50} = 15.87–19.88 μM), ↓spheroid growth, ↓AEBP1, ↓TGF-β-induced parameters (↓AEBP1, ↓p-Akt, ↓ cell proliferation, ↓spheroid growth), synergy with SHP099 In vivo (1123, orthotopic): ↓tumor growth, ↑survival, ↓p-Akt, ↓AEBP1, ↓Ki67, ↓Nestin	↓p-Akt	[24]

 doi:10.20944/preprints202412.1292.v1

Type	Compound	Cell line	Concentration	Biological effects	Effects on cell signaling	Ref.
	MCL3	G442, U87, U251, Hs683	3–30 μM 10, 20, and 40 mg/kg, p.o. (14 times)	In vitro: Cytotoxicity ($IC_{50}^{(96\ h)}$ = 6.44–18.90 μM), ↑PS externalization, ↓IL6, ↓HIF-1α, ↓MMP-2, ↓Bcl-2, ↓Mcl-1 In vivo (G442, heterotopic): ↓tumor volume, ↓tumor weight, ↓PCNA, ↓CD34 (angiogenesis), ↓IL6	↓p-NF-κB, ↓nuclear p-NF-κB, ↓p-STAT3, ↓nuclear p-STAT3	[58]
	Dehydrocostus lactone (DCL)	U118, U251, U87	1–100 μM 10 and 20 mg/kg, i.p. (14 times)	In vitro: Cytotoxicity ($IC_{50}^{(48\ h)}$ = 17.16–26.42 μM), ↓clonogenicity, ↓migration, ↑cytoC, ↑Bax/Bcl-2, ↓COX-2, ↓p300/p50/p65 NF-κB nuclear translocation, ↓p300/p50/p65 NF-κB binding to COX-2 promoter In vivo (U87, heterotopic): ↓tumor volume, ↓tumor weight, ↓COX-2, ↓p-p65, ↓p-IKKβ In vivo (BBB permeability): effectively accumulated in brain tissue	↓p-IKKα/β, ↓p-IκBα, ↓p-p65, ●IKKβ (MolDock)	[18]
	Brevilin A (BVA)	U87, U373, LN229	5–80 μM	Cytotoxicity ($IC_{50}^{(24\ h)}$ = 30–40 μM), ↑PS externalization, ↑ROS, ↓GSH, ↑Bak, ↓Bcl-xl, ↑cytoC, ↓$\Delta\psi_M$, ↑cleaved caspase-3/9, ↑cleaved PARP, ↓XIAP	↓p-JNK, ↓p-p38	[59]
	Xanthatin (XTN)	C6, U251	1–15 μM 10, 20 and 40 mg/kg, i.p. (ND)	In vitro: Cytotoxicity ($IC_{50}^{(24\ h)}$ ~ 15 μM), ↑PS externalization, ↑TUNEL-positive cells, ↑cleaved caspase-3, ↑Bax/Bcl-2, ↑ER stress (↑GRP78, ↑XBP1s, ↑nuclear translocation of CHOP) In vivo (C6, heterotopic): ↓tumor weight, ↑necrotic areas, ↑p-IRE1, ↑ATF6, ↑p-EIF2α, ↑XBP1s, ↑ATF4, ↑CHOP, ↑cleaved caspase-3	↑p-IRE1α, ↑p-EIF2α, ↑ATF4	[60]
		C6, U251	1–15 μM 10, 20 and 40 mg/kg, i.p. (14 times)	In vitro: Cytotoxicity ($IC_{50}^{(12\ h)}$ ~ 15 μM), ↓PCNA, ↓clonogenicity, ↑cleaved PARP, ↑cleaved caspase-3, ↓LC3-II/LC3-I, ↓autophagosome formation, ↑p62, ↓Beclin-1, ↓*BECN1*, ↓*ATG5*, ↓*ATG7*, ↓*ATG12* In vivo (ND, ND): ↓LC3-II/LC3-I, ↑p62, ↑Beclin-1, ↑p-Akt, ↑p-mTOR, ↓p-ULK1	↑p-Akt, ↑p-mTOR, ↓p-ULK1, no effect on p-ERK1/2, p-JNK, and p-p38	[61]
	Lactucopicrin (LPN)	U87	1–10 μM	Cytotoxicity ($IC_{50}^{(24\ h)}$ = 12.5±1.1 μM), ↓clonogenicity, ↓migration, autophagy induction (↓p62, ↑LC3-II, rearrangement of vimentin and α-tubulin cytoskeleton), G_2/M arrest, ↑p53, ↓pro-caspase-6, ↑cleaved PARP, synergy with temozolomide (TMZ)	↓p-Akt, ↓p-ERK1/2, ↑p21, ↓CDK2, ↓p65 NF-κB	[22]

 doi:10.20944/preprints202412.1292.v1

Type	Compound	Cell line	Concentration	Biological effects	Effects on cell signaling	Ref.
	Tomentosin (TTN)	U87	5–100 μM	Cytotoxicity ($IC_{50}^{(48\ h)}$ = 28.8 μM), ↑*BAX*, ↑*CASP3*, ↑*CASP8*, ↑*CASP9*, ↑*CYCS*, ↑*FADD*, ↑*TNF*, ↑*TNFR1*, ↑*TNFR2*, ↑*TIMP2*, ↓clonogenicity	ND	[62]
	Cynaropicrin (CPN)	U87	4–10 μM	ROS-dependent cytotoxicity ($IC_{50}^{(48\ h)}$ = 12.8±3.3), ↓clonogenicity, ↑ROS, ↓$\Delta\psi_M$, ↑cytoC, ↓pro-caspase-9/3, ↑LC3-II/I, ↓p62, ↑senescence (↑β-gal-positive cells), additive effect with TMZ	↓p-ERK, ↓p-p65 NF-κB, ↑nuclear translocation of Nrf2	[63]
	Cynaropicrin (CPN) Dehydrocstus lactone (DCL) Saussureamine B (SAB)	U251 CSCs, U251	ND	Cytotoxicity (U251 CSCs: IC_{50} = 7.9–20.4 μM; U251: IC_{50} = 4.0–10.9 μM)	ND	[88]
	Arglabin diethyl cyanomethylphosphonate (8d) (ADCMP)	T98G	ND	Cytotoxicity ($IC_{50}^{(48\ h)}$ = 16.9±1.3 μM), selectivity index = 3.2	ND	[89]
	9-Oxomicheliolide (OMCL)	U87	ND	Cytotoxicity (IC_{50} = 13.15 μM), ↑PS externalization	ND	[64]
Endoperoxide-containing STLs	Dihydroartemisinin (DAMN)	GL261 GL261 GSCs	10–80 μM	Cytotoxicity (GL261: $IC_{50}^{(24\ h)}$ ~ 80 μM, GL261 GSCs: $IC_{50}^{(24\ h)}$ ~ 40 μM), ↓spheroid growth, G_1 arrest, ↑cleaved caspase-3	↓p-Akt	[67]
		U87	5–160 μM	Cytotoxicity (IC_{50} ~ 70 μM), ↓migration, ↓invasion, ↓ADAM17	↓p-EGFR, ↓p-Akt	[90]
		LN-229, LN-Z308, T269	5–9 μM	Cytotoxicity, ↓clonogenicity, synergy with TMZ, ↑ROS, ↑CAT, ↑GPX1, ↑GPX4, ↑SOD2, ↑LC3-II, ↓Sox2, ↓Nestin	ND	[91]
		U87, U251	50–600 μM 2, 10, and 50 mg/kg, p.o. (45 times)	In vitro: Cytotoxicity ($IC_{50}^{(24\ h)}$ = 200–210 μM), ↓migration, ↓invasion, ↓MMP9, ↓MMP9 activity, ↓MMP7, ↓MMP7 activity, ↑ROS, ↑p53, ↑p-p53 In vivo (U87, U251, heterotopic): ↓tumor volume	↓EGFR, ↓β-catenin, ↓p-β-catenin	[76]
		U87, U251	3.125–200 μM 100 mg/kg, i.p. (28 times)	In vitro: Cytotoxicity ($IC_{50}^{(24\ h)}$ = 16.12–25.05 μM), ↓DNA synthesis, ↓clonogenicity, S and G_2/M arrest, ↑PS externalization, ↑caspase-3, ↑cleaved caspase-3/9, ↑cleaved PARP, ↓$\Delta\psi_M$, ↓glucose uptake, ↓L-lactate, ↓glycolytic capacity, synergy with TMZ, ↓spheroid formation	↓*PGC-1α*, ●ERRα (MolDock, TR-FRET)	[68]

 doi:10.20944/preprints202412.1292.v1

Type	Compound	Cell line	Concentration	Biological effects	Effects on cell signaling	Ref.
				In vivo (U87, orthotopic): ↑median survival time, ↑caspase-3		
	Artesunate (AST)	LN229, A172	15 μM	Senolytic activity: ↓proliferation of senescent cells, ↑PS externalization in senescent cells. Non-toxic for non-senescent cells.	ND	[69]
Other	3 (смотри 3)	U251, C6	1–100 μM	Cytotoxicity (IC_{50} = 36.6–41.6 μM), ↑activated caspases, ↑sub-G_0/G_1, ↑PS externalization, ↑ROS, ↓$\Delta\psi_M$	ND	[72]
	4 (смотри 6)	U251	5–8 μM 2 mg/kg, p.o. (14 times)	In vitro: Cytotoxicity (IC_{50} = 1.7 μM), mitotic catastrophe, ↓c-Myc, ↓Bcl-2, ↓Mcl-1, ↓Bcl-xl, ↓spheroid growth, ↑spheroid cell disaggregation, ↓migration from the spheroid, ↓Hsp105, ↓vimentin, ↓TNAP2, ↓G6PD, ↓GCN1, ↓TrxR1 In vivo (U251, heterotopic): ↓tumor volume, ↓p-STAT3, ↓STAT3	↓STAT3 DNA-binding activity, ↓p-STAT3, ●STAT3 (NMR, MolDock)	[73]
	Goyazensolide (GZD)	U87, T98G	10–100 μM	Cytotoxicity (IC_{50} ~ 6 μM), ↓clonogenicity, no effect on migration, ↑apoptosis, ↑cleaved caspase-3	ND	[70]
	Deoxyelephantopin (DEN)	GL261	0.5–2 μg/mL 10 mg/kg, p.o. (14 times)	In vitro: Cytotoxicity ($IC_{50}^{(24\ h)}$ ~ 2 μg/mL), ↑PS externalization, G_2/M arrest, ↓VEGF, ↓TGF-β, ↑caspase-3, ↑Bax/Bcl-2, ↑cytoC In vivo (GL261, heterotopic): ↓tumor volume, ↓tumor weight, ↑survival	↓CDK4, ↓cyclin D2, ↓p-Akt, ↓p-STAT	[71]
	Enhydrin (EHN)	U87, LN229	2–8 μM 15–25 μM, intracraneal	In vitro: Cytotoxicity ($IC_{50}^{(24\ h)}$ = 1.6–2.6 μM), ↓migration, ↓invasion, ↓N-cadherin, ↓vimentin, ↑E-cadherin In vivo (ND, orthotopic): ↓tumor size, ↑survival, ↓Ki67, ↓Jun, ↓TGF-β1, ↑Smad7	↓Jun, ↓TGF-β1, ↓p-Smad2, ↓nuclear p-Smad2, ↓p-Smad3, ↓nuclear p-Smad3, ↑Smad7	[92]

[1]i.p. – intraperitoneal; [2]ND – no data; [3]● – direct interaction of STLs with protein targets; [4]$\Delta\psi_M$ – mitochondrial membrane potential; [5]p.o. – per oral

 doi:10.20944/preprints202412.1292.v1

Considering the close association of mitochondrial imbalance with reactive oxygen species (ROS) hyperproduction [93], a significant part of the published work reported the ability of STLs to induce oxidative stress in glioblastoma cells (Figure 2B). High stimulatory activity for ROS hyperproduction was found for germacranolides (elephantopinolide A [50], costunolide [51], molephantin [52], DMAPT-D6 [48]), guaianolides (DMAMCL [55,57], brevilin A [59], cynaropicrin [63]), dihydroartemisinin [76,91], and lactone 3 [72]. In addition, molephantin and elephantopinolide A significantly increased mitochondrial ROS production [50,52] and the latter also induced massive lipid peroxidation in U87 cells [50]. Note that blockade of oxidative stress by N-acetylcysteine, a known ROS scavenger, significantly reduced the pro-apoptotic effect of costunolide [51], molephantin [52], DMAPT-D6 [48] and DMAMCL [57], suggesting the critical importance of ROS hyperproduction for the anti-glioblastoma potential of STLs.

Oxidative stress induced by STLs in glioblastoma cells was accompanied by depletion of intracellular glutathione (GSH) [59] and activation of compensatory cytoprotective mechanisms, including upregulation of Nrf2, a key transcription factor regulating cellular defense against oxidative insults [94], induced by DMAPT-D6 [48] and DMAMCL [57], and cynaropicrin-stimulated enhancement of Nrf2 nuclear translocation in U87 cells [63]. Furthermore, a number of STLs led to the overexpression of key Nrf2-dependent antioxidant proteins in glioblastoma cells, namely NADPH oxidase 1 (NOX1), thioredoxin (TrX), heme oxygenase 1 (HO1) and superoxide dismutase 2 (SOD2) by DMAMCL [57] and catalase (CAT), glutathione peroxidases 1 and 4 (GPX1/4) and SOD2 by dihydroartemisinin [91]. Interestingly, costunolide conversely inhibited the expression of Nrf2 on the background of a pronounced pro-oxidant effect in glioblastoma cells [51], and lactone 4 was shown to down-regulate the expression of thioredoxin reductase 1 (TrxR1) [73], which may indicate the ability of STLs to modulate the complex system of negative feedback loops involved in the antioxidant response in glioblastoma cells [95]. Considering the higher susceptibility of brain to oxidative stress compared to other organs [96] and the cellular redox imbalance found in glioblastoma cells [97], the demonstrated ability of STLs to induce ROS hyperproduction due to disruption of mitochondrial homeostasis in glioblastoma cells (Figure 2B) can be exploited for the development of novel anti-glioblastoma drug candidates.

2.3.3. Effect of STLs on Energy Metabolism of Glioblastoma Cells

In addition to the detrimental effect of STLs on mitochondrial homeostasis leading to impairment of oxidative phosphorylation [98], a number of STLs have been found to inhibit glucose metabolism [21,47,51], confirming the ability of STLs to suppress glioblastoma cell viability also by disrupting their energy system (Figure 2B). Ahmad et al. found that costunolide significantly retarded the pentose phosphate pathway in A172 and U87 glioblastoma cells and reduced the expression of its two main enzymes, glucose-6-phosphate dehydrogenase (G6PD) and transketolase (TKT) [51]. Consistent with these results, Guo et al. confirmed the ability of DMAMCL to suppress not only the pentose phosphate pathway, but also anaerobic glycolysis in U118 cells, as evidenced by the significant decrease in intracellular levels of lactate, glucose-6-phosphate, and sedoheptulose-7-phosaphate after DMAMCL treatment, as well as the down-regulation of the expression of genes encoding key glycolytic enzymes [21]. The revealed inhibitory potency of DMAMCL with respect to anaerobic metabolism in U118 cells was found to be mediated by the direct interaction of micheliolide, a major metabolite of DMAMCL, with pyruvate kinase M2 (PKM2), resulting in the increase of pyruvate kinase activity and subsequent suppression of lactate production in glioblastoma cells [21]. Interestingly, parthenolide dimer 4 was also found to bind directly to PKM2 and induce its activity in U87 and U118 cells [47], which may demonstrate the PKM2 targeting potential of different STLs independent of their structure, which requires further studies. Given the involvement of PKM2 not only in metabolic regulation, but also in the control of mitochondrial dynamics and mitochondrial membrane permeability [99], direct interaction of STLs with PKM2, along with the inhibitory effect on energy metabolism, may underlie the STL-induced mitochondrial dysfunction in glioblastoma cells discussed above.

 doi:10.20944/preprints202412.1292.v1

2.3.4. Effect of STLs on Other Processes Associated with Glioblastoma Cell Proliferation

Propidium iodide staining of STL-treated glioblastoma cells clearly demonstrated that the anti-glioblastoma potential of STLs was not only determined by apoptosis induction, but also by suppression of cell proliferation through cell cycle arrest (Table 1). Interestingly, this effect was not limited by the influence of these compounds on a specific cell cycle phase. It was shown that STLs led to accumulation of glioblastoma cells in three different cell cycle phases, namely G0/G1 arrest after treatment with alantolactone [65] and lactone 2 [49], S arrest induced by molephantin [52] and DMAPT-D6 [48], and G2/M arrest induced by parthenolide [46], DMAMCL [57], lactucopicrin [22] and deoxyelephantopin [71]. Interestingly, dihydroartemisinin blocked all of these cell cycle phases [67,68], which may be explained by the cellular context. The cell cycle inhibitory effect of STLs was determined by their modulation of the expression of key regulators of cell cycle phase transition, including down-regulation of cyclin-dependent kinases (CDK1 [48], CDK2 [22,46,48,52,57], CDK4 [52,65,71])), cyclins (cyclin B [48,57], cyclin E [48], cyclin D1 [65], cyclin D2 [71]), and the checkpoint kinase Chk2 [46], as well as upregulation of the cyclin-dependent kinase inhibitors p21 [22,52] and p27 [48] (Figure 2B).

Consistent with the cell cycle-targeting effect of STLs (Table 1) and the known association of cell cycle arrest with cell senescence [100], a number of research groups demonstrated the ability of STLs to induce senescence of glioblastoma cells. Ahmad et al [51] and Rotondo et al [63] demonstrated a significant increase in β-galactosidase activity, a classical senescence inducer [101], in glioblastoma cells treated with costunolide and cynaropicrin, respectively. Moreover, the senescence-inducing effect of costunolide was accompanied by intracellular accumulation of glycogen and a marked decrease in telomerase activity [51]. Interestingly, artesunate, which was not tested for its effect on glioblastoma cell senescence, significantly decreased the viability of temozolomide-induced senescent LN299 and A172 cells showing high senolytic activity [69]. Since senescence is currently considered not only as a glioblastoma-suppressing mechanism due to its arresting effect on cell proliferation [102], but also as a factor promoting glioblastoma progression [103], further detailed studies on the senescence-modulating effect of STLs in glioblastoma cells are required.

In addition to apoptosis induction and cell cycle arrest, the anti-glioblastoma activity of STLs may also be determined by their effect on autophagy (Figure 2B). Pathenolide, lactucopicrin, cynaropicrin, dyhydroartemisinin and molephantin were found to increase the lipidated form of microtubule-associated protein 1 light chain 3 (LC3-II) in glioblastoma cells [22,46,52,63,91], and this process was accompanied by down-regulation of the autophagic substrate p62 [22,63], extensive cytoplasmic vacuolization [46], and strong rearrangement of the vimentin and α-tubulin cytoskeleton [22]. Notably, despite its stimulatory effect on LC3-II, molephantin blocked autophagic flux and caused autophagosome accumulation in glioblastoma cells due to the defect in autophagosome-lysosome fusion [52]. Consistent with molephantin, xanthatin was also found to inhibit autophagic flux in glioblastoma cells, but its effect on autophagy was strictly negative with high accumulation of LC-I, inhibition of autophagosome formation and expression of key autophagic regulators including Beclin-1, ATG5, ATG7 and ATG12 [61], demonstrating a compound-dependent effect of STLs on autophagy. Interestingly, despite the reported anti-autophagic effect, xanthatin induced endoplasmic reticulum (ER) stress in the same cell model, increasing the expression of its key markers, including GRP78, XBP1, CHOP, and ATF4, and enhancing IRE-1α and EIF2α phosphorylation [60]. Given the known association of ER stress with autophagy [104] and its potential as a promising target for glioblastoma therapy [105], the effect of STLs on both autophagy and ER stress requires further detailed studies.

The multidirectional effects of STLs against glioblastoma cells described above were mediated by their blocking effect on a number of key signaling pathways, including NF-κB [18,22,49,53,57,58,63,65], STAT3 [15,47,58,71,73], PI3K/Akt/mTOR [22,24,52,56,63,67,71,90], EGFR [76,86,90], and MAPK [22,59] pathways, which play a critical role in glioblastoma pathogenesis [106]. This complex effect determines the possibility of using STLs not only as individual drug candidates, but also as components of polychemotherapy regimens for glioblastoma. Indeed, marked cytotoxic synergy in glioblastoma cells has been demonstrated for combinations of lactucopicrin or

 doi:10.20944/preprints202412.1292.v1

dihydroartemisinin with temozolomide [22,68,91] and DMAMCL with cisplatin [56], SHP2 inhibitor SHP099 [24] and X-ray treatment [55].

2.4. Permeability of STLs Through Blood-Brain Barrier

The blood-brain barrier (BBB) plays a critical role in maintaining central nervous system (CNS) homeostasis, allowing essential molecules to enter brain tissue and protecting the brain from potentially harmful substances and exogenous xenobiotics [107]. This function of the BBB defines a significant challenge for the treatment of neurological diseases, as effective CNS therapeutics must be able to cross the BBB to reach their intended targets in the brain [108]. Confirming a high anti-glioblastoma potential, a large number of reports have demonstrated the ability of many STLs to effectively cross the BBB using various relevant models. For example, chemoinformatics tools predicted the BBB permeability of ambrosin, artemisinin, and deoxyelephantopin [109–111], and in vitro assays, including transwell penetration through HBMEC or MDCK monolayers and the parallel artificial membrane permeation assay (PAMPA), showed a high BBB penetration potential of parthenolide [112] and its dimer [47], costunolide [112], goyazenolide [70], lychnofolide [70] and a 6-*O*,*O*-diacetylbritannilactone [113]. More informative data were obtained in vivo by LC-MS/MS or positron emission tomography analysis of animal brain tissue after STLs injections, demonstrating successful BBB permeability of DMAPT [81,82], alantolactone [65], DMAMCL [54], and dehydrocostus lactone [18]. In addition, as indirect evidence of brain accumulation of STLs, we can also consider the effective blocking of orthotopic glioblastoma tumor growth by a series of germacranolides [82], eudesmanes [86], guaianolides [15,24,54,57], dihydroartemisinin [68], and enhydrin [92], as well as the high neuroprotective potential in vivo of parthenolide [114] and alantolactone [115]. Thus, the accumulated data indicate the feasibility of using STLs as a platform for the development of novel anti-glioblastoma drug candidates.

2.5. Anti-Glioblastoma Efficacy of STLs In Vivo

The pronounced multi-target inhibitory activity of STLs observed in glioblastoma cells in vitro has been extensively verified in glioblastoma mouse models (Table 1). STLs administered intraperitoneally or orally at doses of 5-200 mg/kg were found to effectively block tumor growth in heterotopic glioblastoma xenograft models in mice, demonstrating high antitumor efficacy with a median inhibition rate of 66.5% (Figure 2C). The top 5 most active STLs included costunolide, DMAMCL, MCL3, alantolactone, and xanthatin, which suppressed tumor growth by 95% [51], 81.5% [54], 79% [58], 70.5% [65], and 69% [60], respectively, compared to control (Figure 2C). Other STLs that inhibited subcutaneous glioblastoma growth were deoxyelephantopin [71], dehydrocostus lactone [18], molephantin [52], dihydroartemisinin [76], and lactones 2 [49] and 4 [73], with inhibition rates ranging from 26.2% to 66.5% (Figure 2C). The pronounced antitumor effect of these compounds was accompanied by the absence of organ and brain toxicity, decrease in cell proliferation [58], and activation of apoptosis in glioblastoma tissues [47,51,52,60]. In addition, xanthatin and MCL3 increase necrosis area [60] and inhibit angiogenesis [58] in xenograft tumors, respectively, demonstrating the complex effect of STLs on glioblastoma growth in vivo. In addition to the high efficacy in the subcutaneous glioblastoma model, STLs were found to significantly increase the survival of mice with orthotopically implanted glioblastoma, as demonstrated for DMAPT [82], alantolactone [86], DMAMCL [15,24,57], dihydroartemisinin [68], and enhydrin [92] (Table 1). This effect was accompanied by marked suppression of tumor growth [24,54,57,86,92], decrease in Ki67 expression [24,57,92], activation of caspase-3 [68], and decrease in infiltration of tumor tissue by pro-tumor M2 macrophages [15]. Taken together, these results clearly confirmed the high anti-glioblastoma potential of STLs.

2.6. Pharmacological Potential of STLs Against Proneural-Mesenchymal Transition of Glioblastoma Cells

2.6.1. Proneural-Mesenchymal Transition as Promising Target for Glioblastoma Therapy

 doi:10.20944/preprints202412.1292.v1

Proneural-mesenchymal transition (PMT) is a specific type of epithelial-mesenchymal transition (EMT) that occurs in glioblastoma cells and is involved in regulation of their diffuse growth [7,116]. Given the high association of PMT with glioblastoma severity [3] and the known inhibitory potential of STLs against EMT of various epithelial-type tumor cells [23,117–119], a separate chapter of this review is devoted to the effect of STLs on PMT, which has been studied to a much lesser extent. Similar to EMT, PMT is induced in glioblastoma cells by various factors from the tumor microenvironment, including hypoxia [120,121], necrosis [122], therapeutic radiation [123,124], ROS [123], immune cells, including tumor-associated macrophages (TAMs) [124,125] and mesenchymal stem cells (MSCs) [126,127], as well as cytokines and growth factors [128–130]. Both EMT and PMT represent a reversible transformation of cells across a spectrum of phenotypes, rather than a simple dual-state switch, with increasing tumor invasion and metastasis as cells transition toward the mesenchymal state [131,132]. However, because GBM originates from non-epithelial tissues, the extreme points in the PMT spectrum diverge from those in EMT. The transition occurs between the proneural subtype, which expresses DLL3, PDGFRA, OLIG2, and SOX2, and the mesenchymal subtype, which is abundant in CD44, YKL-40, ANXA1, and MET (Figure 3A) [116]. By analyzing the regulatory landscape of PMT, three key elements can be identified, including “hubs”, “regulatory core”, and “stabilizing module”. Two “hubs”, NF-κB and GSK-3β, integrate information from the primary PMT-inducing pathways (Figure 3B). NF-κB is activated in glioblastoma cells by various factors, including mutations in IκBα [133], radiation-induced DNA damage [133], the aldehyde dehydrogenase 1A3 (ALDH1A3) [134], the adhesion molecule CD146 [135], and a number of cytokines, such as CXCL1 [130], chemerin [129], TNF-α [136], and TGF-β [125,128]. Once activated, NF-κB stabilizes C/EBPβ in the “regulatory core” [136] and enhances vasculogenic mimicry of glioblastoma cells by activating the Ephrin-B2/EPHB4 and Notch pathways through the induction of tenascin C (TNC) [137]. The smaller hub, GSK-3β, integrates signals from mutations in NF1 and PTEN [133], as well as from the Wnt [124], sortilin [138], and EGF [139] pathways, playing an important role in glioblastoma pathogenesis. Upon activation, GSK-3β degrades, which stabilizes the β-catenin, known PMT master regulator [140], and induces WISP1, thereby facilitating PMT through the α6β2-integrin pathway [141,142]. Additional pathways supporting PMT of glioblastoma cells are induced by hypoxia [120,121], necrosis [122], 17β-estradiol [143], CXCL12 [144], C5a [127], bradykinin [126] and the interleukin (IL)-6 family cytokines, including IL-6 [145], leukemia inhibitory factor (LIF) [146], and oncostatin M (OSM) [147] (Figure 3B). Transcription factors (TFs) form two “regulatory cores” of PMT, including TAZ/TEAD2 [122,148] and a hierarchical module consisting of C/EBP, STAT3, FOSL2, bHLH-B2, and RUNX1 [149] (Figure 3B). These cores regulate the transcription of proneural and mesenchymal signatures and have nearly non-overlapping sets of regulatory targets [148]. The classical EMT TFs Snail [150], Slug [151], Twist [138], and ZEB1 [127], along with Nrf2 [152] and Fox family TFs FOXD1 [153], FOXM1 [154], and FOXS1 [145], provide additional transregulation of PMT (Figure 3A, B). The “stabilizing module” consisting of the deubiquitinases USP3, USP9X, USP10, USP21, and USP36 maintains PMT by preventing ubiquitin-dependent proteasomal degradation of Snail [150], ALDH1A3 [155], RUNX1 [156], FOXD1 [157], and Slug [158], respectively (Figure 3B).

Preprints.org (www.preprints.org) | NOT PEER-REVIEWED | Posted: 16 December 2024 doi:10.20944/preprints202412.1292.v1

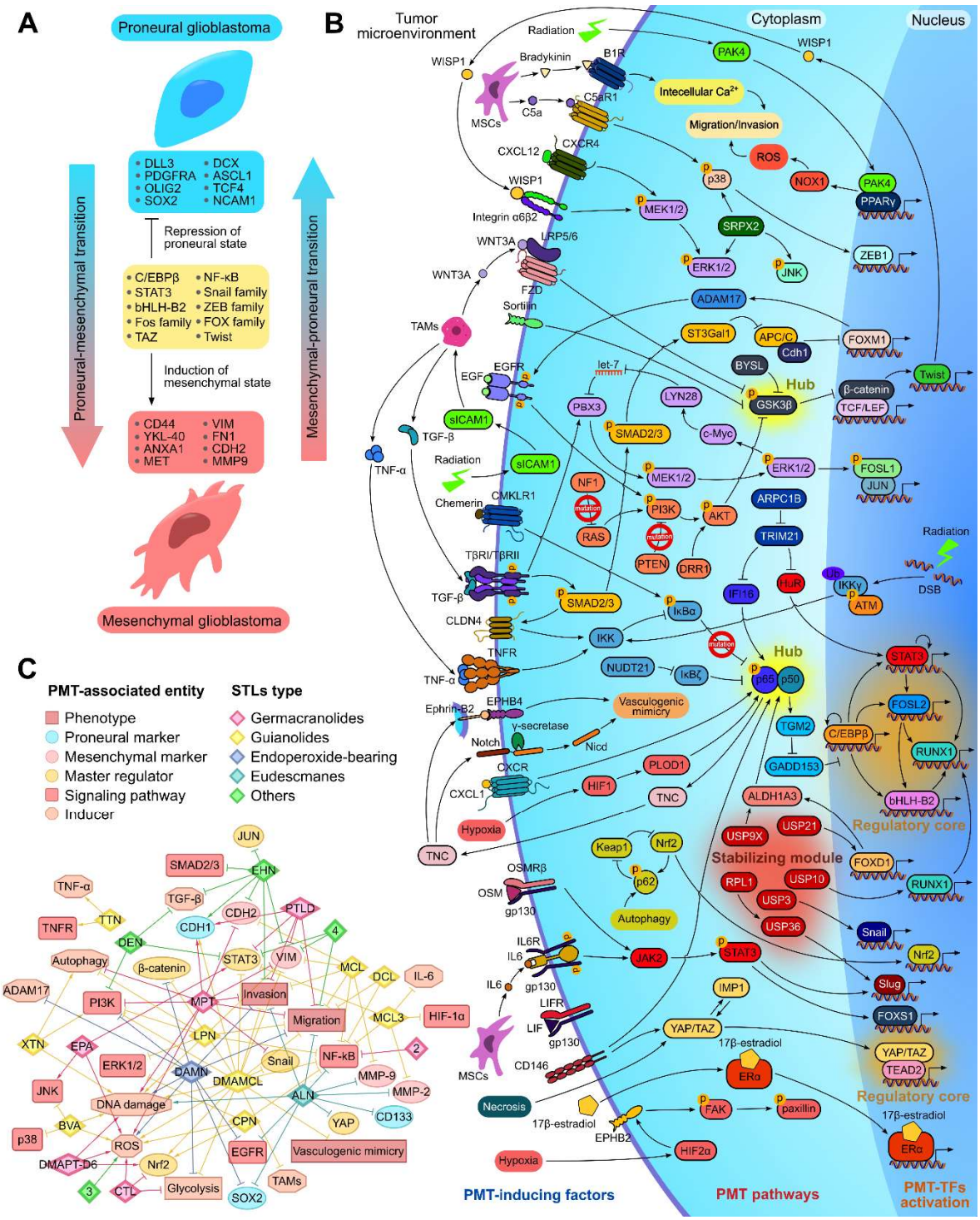

Figure 3. Proneural-mesenchymal transition (PMT) as a target for STLs. (A) Cellular plasticity in glioblastoma. In the tumor microenvironment, glioblastoma cells can switch between proneural and mesenchymal states, which differ in morphology and marker expression. The transition to the mesenchymal state, known as PMT, results in an invasive phenotype and is regulated by a subset of transcription factors (TFs), including both classical EMT TFs such as Slug, Snail, and Twis, and PMT-specific TFs such as TAZ, STAT3, and bHLH-H2. (B) Pathways that induce PMT. Several factors from the tumor microenvironment, including hypoxia, necrosis, inflammation, and soluble growth factors, can induce PMT. These factors activate a complex regulatory network of signaling pathways in which NF-κB and GSK-3β serve as key interconnected "hubs" (shown in yellow). This network ultimately activates PMT TFs, which are organized in a hierarchy with a "regulatory core" of PMT-specific TFs (highlighted in orange) and supporting TFs. In addition, several deubiquitinases form a "stabilizing module" (marked in red) that maintains PMT by extending the half-life of PMT TFs. (C) STLs-PMT

 doi:10.20944/preprints202412.1292.v1

interaction network. Based on a manual literature review, STLs mediate various PMT-associated cell phenotypes, molecular markers, master regulators, signaling pathways, and inducing factors.

PMT inhibition shows promise as a strategy against glioblastoma invasion, but it is still in the pre-clinical phase. Compounds from various chemical classes, including lignins [159], nitroimidazoles [160], flavonoids [161,162], ubiquinones [163], benzanilides [164], quinolones [165], halopyridines [166], benzylamines [155], benzodiazines [156], and thiuram disulfides [157], have been shown to inhibit the motility and invasion of glioblastoma cells *in vitro* and reduce tumor growth in animal xenograft models by targeting key nodes within the PMT regulatory network (Figure 3B). Tetrandrine and DYT-40 target the NF-κB pathway [159,160], while quercetin, nobiletin, and 4-acetylantroquinonol B inhibit signaling pathways linked to GSK-3β, another critical hub in PMT regulation [161–163]. HJC0152, nitidine chloride, and YM155 repress STAT3, which plays a central role in the regulatory core of PMT [164–166]. WP1130, spautin-1, and disulfiram disrupt the stabilization of ALDH1A3, RUNX1, and FOXD1 by inhibiting the deubiquitinases USP9X, USP10, and USP21, respectively [155–157]. All mentioned compounds are considered now as promising anti-glioblastoma drug candidates.

2.6.2. Effect of STLs on Key Regulators of PMT

As shown in Table 1, STLs effectively inhibited the migration and invasion of glioblastoma cells and their spheroidal growth, processes closely associated with PMT [7]. Indeed, many publications demonstrated a significant inhibitory effect of STLs on the NF-κB signaling pathway, which plays a hub role in PMT (Figure 3B). Blockade of NF-κB nuclear translocation and upstream regulators of this process in glioblastoma cells was demonstrated for alantolactone [65], micheliolide [53], DMAMCL [57], MCL3 [58], dehydrocostus lactone [18], lactucopicrin [22], and cynaropicrin [63]. Of note, IKKβ can be considered as a primary target of STLs: using a pull-down assay, Li et al. demonstrated a direct interaction of DMAMCL with IKKβ [57], and alantolactone and dehydrocostus lactone were shown to form a stable complex with IKKβ in molecular docking simulations [18,65]. The second PMT-related hub, GSK3β, was found to be less susceptible to STLs: it was reported that only DMAMCL and dihydroartemisinin effectively inhibited the expression and phosphorylation of β-catenin, a downstream effector of GSK3β, in glioblastoma cells [56,76].

Consistent with the suppression of PMT-associated hubs, STLs effectively modulated the expression of key PMT-associated markers in glioblastoma cells, including down-regulation of vimentin by molephantin [52], parthenolide dimer [47], micheliolide [53], DMAMCL [56], lactone 4 [73], and enhydrin [92], down-regulation of Snail by DMAMCL [56] and N-cadherin by molephantin [52], micheliolide [53], and enhydrin [92], as well as up-regulation of E-cadherin by molephantin [52], parthenolide dimer [47], DMAMCL [56], and enhydrin [92]. In addition, alantolactone, micheliolide, MCL3, and dihydroartemisinin effectively inhibited the expression of mesenchymal type-associated matrix metalloproteinases MMP-2 and MMP-9 [53,58,65,66,76], and alantolactone decreased the expression of YAP [86], an important regulator of PMT [3] (Figure 3C). Interestingly, despite high anti-PMT activity, alantolactone and dihydroartemisinin were found to inhibit the expression of proneural SOX2 and CD133 in glioblastoma cells [86,91], which may indicate the ability of these compounds to affect only specific compartments of the PMT-associated regulome, which requires further investigation.

In addition to inhibiting NF-κB signaling, STLs were found to suppress a number of other signaling axes involved in PMT regulation (Figure 3C), including:

- blockage of STAT3, as shown for parthenolide dimer [47], MCL3 [58], lactone 4 [73], and DMAMCL (moreover, DMAMCL were found to directly interact with STAT3) [15];
- PI3K/Akt/mTOR pathway inhibition by molephantin [52], DMAMCL [24,56], lactucopicrin [22], dihydroartemisinin [67,90], and deoxyelephantopin [71];
- inhibition of MAPK by brevelin A [59], xanthatin [61], lactucopicrin [22], and cynaropicrin [63];
- suppression of EGFR by alantolactone [86] and dihydroartemisinin [90], as well as HIF1α and Smad2/3 by MCL3 [58] and enhydrin [92], respectively.

Preprints.org (www.preprints.org) | NOT PEER-REVIEWED | Posted: 16 December 2024 doi:10.20944/preprints202412.1292.v1

It should be noted that despite the demonstrated effects of STLs on key regulators and processes associated with PMT induction (Figure 3C), published reports have only demonstrated the suppressor effect of STLs on the basal proneural-mesenchymal balance in glioblastoma cells, whereas their effect on PMT induced by relevant stimulators, which is more informative for understanding anti-glioblastoma potency [167], has not been investigated to our knowledge. Only Hou et al. demonstrated the ability of DMAMCL to inhibit TGF-β-induced proliferation and spheroid growth of patient-derived glioblastoma stem cells [24], and enhydrin was found to decrease TGF-β expression during PMT blockade in U87 and LN229 cells [92]. Thus, investigating the effects of STLs on PMT induced by various glioblastoma severity-related factors (e.g., TGF-β, EGF, hypoxia, etc.) remains an extremely important research goal for future work.

2.6.3. The Association of Protein Interactome of STLs with PMT

Finally, to estimate the pharmacological potential of STLs with respect to inductor-mediated PMT, the PMT-related gene association network was reconstructed (Figure 4) from two independent datasets, including (i) proneural and mesenchymal Verhaak gene signatures obtained from patient glioblastoma material characterized by the expression of various glioblastoma severity-associated factors [168], and (ii) direct protein targets of STLs selected from published data (Table 2) (for detailed information on the methods used, see the Supplementary materials).

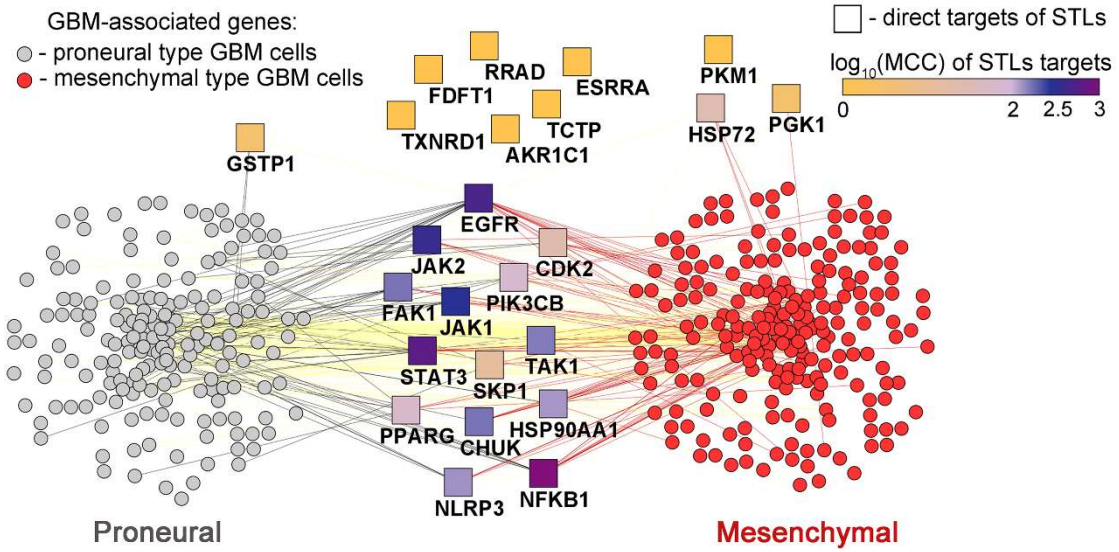

Figure 4. The involvement of direct protein targets of STLs in glioblastoma-related regulome. Proneural and mesenchymal-associated gene signatures were obtained from The Molecular Signatures Database (MSigDB) and shown as gray and red circle nodes, respectively. Experimentally verified primary protein targets of STLs from published data (shown as square nodes) were added to the glioblastoma-related regulome. MCC – the Maximal Clique Centrality (MCC) score of STLs targets within the glioblastoma-related regulome, calculated using the cytoHubba plugin in Cytoscape. Red and black edges indicate interaction of STLs targets with mesenchymal and proneural genes, respectively.

Table 2. Direct protein targets of STLs.

Type	Compound	Protein	Constant, μM	Method	Ref
Endorepoxide-bearing	Artemisinin	MD2	K_D[1] = 2.6	Fluorescence titrations, thermal shift assay	[169]
	Artemisitene	FDFT1	K_D = 165	Thermal shift assay, SPR[2]	[170]
	DAMN	ERRα	-	TR-FRET	[68]

 doi:10.20944/preprints202412.1292.v1

Type	Compound	Protein	Constant, μM	Method	Ref
		PI3K-β	-	Computational approaches	[171]
Eudesmanes	Alantolactone	AKR1C1	K_D = 11.8	SPR, enzyme activity assay	[172]
	Isoalantolactone	STAT3	K_D = 100	Thermal shift assay, SPR	[173]
Germacranolides	Costunolide derivative D5	PKM2	K_D = 0.018	Thermal shift assay, SPR	[174]
	Costunolide	CaMKII	K_D = 21.57	DARTS[3], thermal shift assay	[175]
		CDK2	K_D = 32.02	DARTS, thermal shift assay, SPR	[176]
		TrxR1	-	SPR, enzyme activity assay	[177]
	Elephantopinolide A Cis-scabertopin Elephantopinolide F	GSTP1	-	Thermal shift assay	[178]
	Eupalinolide B	TAK1	-	Thermal shift assay	[179]
	Parthenolide	USP7	-	Thermal shift assay, SPR, enzyme activity assay	[180]
		FAK1	-	Proteomics, enzyme activity assay	[181]
		HSP72	-	LC-MS/MS	[182]
		NFκB	-	EMSA	[183]
		USP47	IC_{50}[4] = 24.97	Thermal shift assay, enzyme activity assay	[184]
	Parthenolide dimer	PKM2	-	Thermal shift assay	[47]
Guianolides and pseudoguaianolides	Arglabin	EGFR	-	Phospho-RTK array	[185]
	Argyinolide S	JAK1	-	DARTS	[186]
	Dehydrocostus lactone	TCTP	K_D = 5.33	SPR	[187]
	DMAMCL	PAI-1	K_D = 2310	Thermal shift assay, SPR, pull-down	[56]
		STAT3	-	Pull-down	[15]
		IKKβ	-	Pull-down, LC-MS/MS	[57]
	Micheliolide	PKM2	-	Pull-down assay	[21]
	1,6-*O*,*O*-diacetylbritannilactone	NLRP3	-	Thermal shift assay	[188]
	Bigelovin	JAK2	IC_{50} = 44.24	Enzyme activity assay	[189]
	Brevilin A	STAT3	K_D = 0.01	SPR	[190]
		IKKα/β	-	Thermal shift assay, LC-MS/MS	[191]
	Britannin	GSK-3β	K_D = 30.1	Enzyme activity assay, SPR	[192]
	Helenalin	NF-κB	K_D = 4.8	SPR	[193]
Others	4	STAT3	-	Nuclear magnetic resonance	[73]
	Arteannuin B	UBE2D3	K_D = 1.2	Thermal shift assay, DARTS, LC-MS/MS	[194]

 doi:10.20944/preprints202412.1292.v1

Type	Compound	Protein	Constant, μM	Method	Ref
	Chloranthalactone B	NLRP3	K_D = 10.3	Pull-down, DARTS, thermal shift assay	[195]
	Deoxyelephantopin	Hsp90α	-	DARTS	[196]
		PPARγ	-	Enzyme activity assay	[197]
	Isodeoxyelephantopin	TrxR1	-	Enzyme activity assay	[198]
	Tatridin A	PGK1	IC_{50} = 3.76	DARTS, enzyme activity assay	[199]

[1]K_D – dissociation constant; [2]SPR – surface plasmon resonance; [3]DARTS – drug affinity responsive target stability; [4]IC_{50} – half maximal inhibitory concentration.

Topological analysis of the obtained interactome clearly confirmed the expediency of further detailed investigation of STLs in stimulated PMT models: more than half of the analyzed direct targets of STLs were found to be associated with PMT signature with high Maximal Clique Centrality (MCC) score (Figure 4), an important topological characteristic demonstrating the hub position of nodes within the evaluated interactome [200]. The top 5 targets of SLTs most associated with PMT gene signature included STAT3, NF-κB, JAK1, JAK2 and EGFR (Figure 4), which is consistent with the data discussed above (Figure 3B,C). The results obtained can be used to design further studies on the anti-PMT activity of STLs. Considering the hub positions of a number of direct targets of STLs, some of the inducer-mediated PMT models can be considered as the most sensitive to STLs and promising for further analysis, including PMT stimulated by EGF (target: EGFR), IL6 (targets: STAT3 and JAKs [201]), IL1 (target: TAK1 [202]), or bacterial toxins (target: NLRP3 inflammasome [203]).

3. Conclusion and Future Perspectives

STLs are multi-target small compounds of natural origin with proven anti-glioblastoma potential. Scientific data accumulated over the last decade demonstrate the ability of STLs to effectively penetrate the BBB and suppress glioblastoma cell proliferation and viability both in vitro and in vivo through massive mitochondrial imbalance with subsequent oxidative stress and apoptosis induction, inhibition of cell energy metabolism, activation of autophagy and cell cycle arrest. In addition, STLs were found to effectively affect the proneural-mesenchymal balance in glioblastoma cells, contributing to their depletion of mesenchymal features, which contributes to the suppression of tumor cell migration and invasion. The bioinformatic analysis performed by us in the framework of this review suggests the need for further investigation of the anti-PMT activity of STLs using inductor-mediated PMT models to more deeply understand the mechanism of their anti-glioblastoma activity.

Supplementary Materials: The following supporting information can be downloaded at the website of this paper posted on Preprints.org, Supplementary materials describing bioinformatics methods used.

Author Contributions: Conceptualization, A.V.M.; methodology, A.V.M.; software, A.V.M., A.D.M. and K.V.O.; validation, A.V.M., A.D.M. and K.V.O.; formal analysis, A.V.M.; investigation, A.V.M., A.D.M. and K.V.O.; resources, A.V.M.; data curation, A.V.M., A.D.M. and K.V.O.; writing—original draft preparation, A.V.M., A.D.M. and K.V.O.; writing—review and editing, A.V.M.; visualization, A.D.M. and K.V.O.; supervision, A.V.M.; project administration, A.V.M.; funding acquisition, A.V.M. All authors have read and agreed to the published version of the manuscript.

Funding: This research was funded by the Russian Science Foundation, grant number 23-14-00374.

Institutional Review Board Statement: Not applicable.

Informed Consent Statement: Not applicable.

Data Availability Statement: Upon reasonable request, the corresponding author will provide the data generated during this study.

Acknowledgments: The authors gratefully thank Daria O. Kichkina for assistance in the initial stages of writing this review.

 doi:10.20944/preprints202412.1292.v1

Conflicts of Interest: The authors declare no conflicts of interest.

References

1. Hawly, J.; Murcar, M.G.; Schcolnik-Cabrera, A.; Issa, M.E. Glioblastoma stem cell metabolism and immunity. *Cancer Metastasis Rev.* **2024**, *43*, 1015–1035, doi:10.1007/s10555-024-10183-w.
2. Torrisi, F.; Alberghina, C.; D'Aprile, S.; Pavone, A.M.; Longhitano, L.; Giallongo, S.; Tibullo, D.; Di Rosa, M.; Zappalà, A.; Cammarata, F.P.; et al. The Hallmarks of Glioblastoma: Heterogeneity, Intercellular Crosstalk and Molecular Signature of Invasiveness and Progression. *Biomedicines* **2022**, *10*, doi:10.3390/biomedicines10040806.
3. Fedele, M.; Cerchia, L.; Pegoraro, S.; Sgarra, R.; Manfioletti, G. Proneural-Mesenchymal Transition: Phenotypic Plasticity to Acquire Multitherapy Resistance in Glioblastoma. *Int. J. Mol. Sci.* 2019, *20*.
4. Chiariello, M.; Inzalaco, G.; Barone, V.; Gherardini, L. Overcoming challenges in glioblastoma treatment: targeting infiltrating cancer cells and harnessing the tumor microenvironment. *Front. Cell. Neurosci.* **2023**, *17*, 1327621.
5. Yalamarty, S.S.; Filipczak, N.; Li, X.; Subhan, M.A.; Parveen, F.; Ataide, J.A.; Rajmalani, B.A.; Torchilin, V.P. Mechanisms of Resistance and Current Treatment Options for Glioblastoma Multiforme (GBM). *Cancers (Basel).* **2023**, *15*, 2116, doi:10.3390/cancers15072116.
6. Lan, Z.; Li, X.; Zhang, X. Glioblastoma: An Update in Pathology, Molecular Mechanisms and Biomarkers. *Int. J. Mol. Sci.* **2024**, *25*, 3040, doi:10.3390/ijms25053040.
7. Lai, Y.; Lu, X.; Liao, Y.; Ouyang, P.; Wang, H.; Zhang, X.; Huang, G.; Qi, S.; Li, Y. Crosstalk between glioblastoma and tumor microenvironment drives proneural–mesenchymal transition through ligand-receptor interactions. *Genes Dis.* **2024**, *11*, 874–889, doi:https://doi.org/10.1016/j.gendis.2023.05.025.
8. Kalya, M.; Beißbarth, T.; Kel, A.E. Master Regulators Associated with Poor Prognosis in Glioblastoma Multiforme. *Biochem. (Moscow), Suppl. Ser. B Biomed. Chem.* **2021**, *15*, 263–273, doi:10.1134/S1990750821040077.
9. Koehler, A.; Karve, A.; Desai, P.; Arbiser, J.; Plas, D.R.; Qi, X.; Read, R.D.; Sasaki, A.T.; Gawali, V.S.; Toukam, D.K.; et al. Reuse of Molecules for Glioblastoma Therapy. *Pharmaceuticals* **2021**, *14*, 99, doi:10.3390/ph14020099.
10. Daher, A.; Kesari, S. Chapter 14 - Repurposing drugs in glioblastoma. In; Vitorino, C., Balaña, C., Cabral, C.B.T.-N.I.I.G., Eds.; Academic Press, 2023; pp. 285–317 ISBN 978-0-323-99873-4.
11. Xu, F.; Yang, Y.-H.; Yang, H.; Li, W.; Hao, Y.; Zhang, S.; Zhang, Y.-Z.; Cao, W.-X.; Li, X.-X.; Du, G.-H.; et al. Progress of studies on natural products for glioblastoma therapy. *J. Asian Nat. Prod. Res.* **2024**, *26*, 154–176, doi:10.1080/10286020.2023.2300367.
12. Wang, X.; Meng, F.; Mao, J. Progress of natural sesquiterpenoids in the treatment of hepatocellular carcinoma. *Front. Oncol.* **2024**, *14*, 1445222.
13. Cao, F.; Chu, C.; Qin, J.-J.; Guan, X. Research progress on antitumor mechanisms and molecular targets of Inula sesquiterpene lactones. *Chin. Med.* **2023**, *18*, 164, doi:10.1186/s13020-023-00870-1.
14. Paço, A.; Brás, T.; Santos, J.O.; Sampaio, P.; Gomes, A.C.; Duarte, M.F. Anti-Inflammatory and Immunoregulatory Action of Sesquiterpene Lactones. *Molecules* **2022**, *27*, 1142, doi:10.3390/molecules27031142.
15. Tong, L.; Li, J.; Li, Q.; Wang, X.; Medikonda, R.; Zhao, T.; Li, T.; Ma, H.; Yi, L.; Liu, P.; et al. ACT001 reduces the expression of PD-L1 by inhibiting the phosphorylation of STAT3 in glioblastoma. *Theranostics* **2020**, *10*, 5943–5956, doi:10.7150/thno.41498.
16. Laurella, L.C.; Mirakian, N.T.; Garcia, M.N.; Grasso, D.H.; Sülsen, V.P.; Papademetrio, D.L. Sesquiterpene Lactones as Promising Candidates for Cancer Therapy: Focus on Pancreatic Cancer. *Molecules* **2022**, *27*, 3492, doi:10.3390/molecules27113492.
17. Matos, M.S.; Anastácio, J.D.; Dos Santos, C.N. Sesquiterpene lactones: Promising natural compounds to fight inflammation. *Pharmaceutics* **2021**, *13*, 991, doi:10.3390/pharmaceutics13070991.
18. Wang, J.; Yu, Z.; Wang, C.; Tian, X.; Huo, X.; Wang, Y.; Sun, C.; Feng, L.; Ma, J.; Zhang, B.; et al. Dehydrocostus lactone, a natural sesquiterpene lactone, suppresses the biological characteristics of glioma, through inhibition of the NF-κB/COX-2 signaling pathway by targeting IKKβ. *Am. J. Cancer Res.* **2017**, *7*, 1270–1284.
19. Yan, X.; Bai, M.; Yao, G.; Wang, X. Research progress on anti-glioma mechanism of natural sesquiterpene lactones. *Chinese J. Clin. Pharmacol. Ther. 29*, 1174–1184.
20. Abu-Izneid, T.; Rauf, A.; Shariati, M.A.; Khalil, A.A.; Imran, M.; Rebezov, M.; Uddin, M.S.; Mahomoodally, M.F.; Rengasamy, K.R.R. Sesquiterpenes and their derivatives-natural anticancer compounds: An update. *Pharmacol. Res.* **2020**, *161*, 105165, doi:https://doi.org/10.1016/j.phrs.2020.105165.
21. Guo, J.; Xue, Q.; Liu, K.; Ge, W.; Liu, W.; Wang, J.; Zhang, M.; Li, Q.; Cai, D.; Shan, C.; et al. Dimethylaminomicheliolide (DMAMCL) Suppresses the Proliferation of Glioblastoma Cells via Targeting Pyruvate Kinase 2 (PKM2) and Rewiring Aerobic Glycolysis. *Front. Oncol.* **2019**, *9*, 993.

22. Rotondo, R.; Oliva, M.A.; Staffieri, S.; Castaldo, S.; Giangaspero, F.; Arcella, A. Implication of Lactucopicrin in Autophagy, Cell Cycle Arrest and Oxidative Stress to Inhibit U87Mg Glioblastoma Cell Growth. *Molecules* **2020**, *25*, 5843, doi:10.3390/molecules25245843.
23. Ma, J.-H.; Qi, J.; Liu, F.-Y.; Lin, S.-Q.; Zhang, C.-Y.; Xie, W.-D.; Zhang, H.-Y.; Li, X. Ivalin Inhibits Proliferation, Migration and Invasion by Suppressing Epithelial Mesenchymal Transition in Breast Cancer Cells. *Nutr. Cancer* **2018**, *70*, 1330–1338, doi:10.1080/01635581.2018.1539185.
24. Hou, Y.; Sun, B.; Liu, W.; Yu, B.; Shi, Q.; Luo, F.; Bai, Y.; Feng, H. Targeting of glioma stem-like cells with a parthenolide derivative ACT001 through inhibition of AEBP1/PI3K/AKT signaling. *Theranostics* **2021**, *11*, 555–566, doi:10.7150/thno.49250.
25. Moujir, L.; Callies, O.; Sousa, P.M.C.; Sharopov, F.; Seca, A.M.L. Applications of sesquiterpene lactones: A review of some potential success cases. *Appl. Sci.* **2020**, *10*, doi:10.3390/app10093001.
26. Hsu, C.-Y.; Rajabi, S.; Hamzeloo-Moghadam, M.; Kumar, A.; Maresca, M.; Ghildiyal, P. Sesquiterpene lactones as emerging biomolecules to cease cancer by targeting apoptosis. *Front. Pharmacol.* **2024**, *15*, 1371002.
27. Schmidt, T.J. Structure-Activity Relationships of Sesquiterpene Lactones. In *Studies in Natural Products Chemistry*; Atta-ur-Rahman, B.T., Ed.; Elsevier, 2006; Vol. 33, pp. 309–392 ISBN 1572-5995.
28. Patrushev, S.S.; Rybalova, T. V.; Ivanov, I.D.; Vavilin, V.A.; Shults, E.E. Synthesis of a new class of bisheterocycles via the Heck reaction of eudesmane type methylene lactones with 8-bromoxanthines. *Tetrahedron* **2017**, *73*, 2717–2726, doi:10.1016/j.tet.2017.03.016.
29. Liu, X.; Bian, L.; Duan, X.; Zhuang, X.; Sui, Y.; Yang, L. Alantolactone: A sesquiterpene lactone with diverse pharmacological effects. *Chem. Biol. Drug Des.* **2021**, *98*, 1131–1145, doi:https://doi.org/10.1111/cbdd.13972.
30. De Ford, C.; Ulloa, J.L.; Catalán, C.A.N.; Grau, A.; Martino, V.S.; Muschietti, L. V.; Merfort, I. The sesquiterpene lactone polymatin B from Smallanthus sonchifolius induces different cell death mechanisms in three cancer cell lines. *Phytochemistry* **2015**, *117*, 332–339, doi:10.1016/j.phytochem.2015.06.020.
31. Chen, Y.-L.; Xiong, L.-A.; Ma, L.-F.; Fang, L.; Zhan, Z.-J. Natural product-derived ferroptosis mediators. *Phytochemistry* **2024**, *219*, 114002, doi:https://doi.org/10.1016/j.phytochem.2024.114002.
32. Lim, C.B.; Fu, P.Y.; Ky, N.; Zhu, H.S.; Feng, X.L.; Li, J.; Srinivasan, K.G.; Hamza, M.S.; Zhao, Y. NF-κB p65 repression by the sesquiterpene lactone, Helenalin, contributes to the induction of autophagy cell death. *BMC Complement. Altern. Med.* **2012**, *12*, 1–12, doi:10.1186/1472-6882-12-93.
33. Yang, R.; Ma, S.; Zhuo, R.; Xu, L.; Jia, S.; Yang, P.; Yao, Y.; Cao, H.; Ma, L.; Pan, J.; et al. Suppression of endoplasmic reticulum stress-dependent autophagy enhances cynaropicrin-induced apoptosis via attenuation of the P62/Keap1/Nrf2 pathways in neuroblastoma. *Front. Pharmacol.* **2022**, *13*, 977622, doi:10.3389/fphar.2022.977622.
34. Tabata, K.; Nishimura, Y.; Takeda, T.; Kurita, M.; Uchiyama, T.; Suzuki, T. Sesquiterpene lactones derived from Saussurea lappa induce apoptosis and inhibit invasion and migration in neuroblastoma cells. *J. Pharmacol. Sci.* **2015**, *127*, 397–403, doi:https://doi.org/10.1016/j.jphs.2015.01.002.
35. Kim, M.Y.; Lee, H.; Ji, S.Y.; Kim, S.Y.; Hwangbo, H.; Park, S.-H.; Kim, G.-Y.; Park, C.; Leem, S.-H.; Hong, S.H.; et al. Induction of Apoptosis by Isoalantolactone in Human Hepatocellular Carcinoma Hep3B Cells through Activation of the ROS-Dependent JNK Signaling Pathway. *Pharmaceutics* **2021**, *13*, 1627, doi:10.3390/pharmaceutics13101627.
36. Güçlü, E.; Çınar Ayan, İ.; Dursun, H.G.; Vural, H. Tomentosin induces apoptosis in pancreatic cancer cells through increasing reactive oxygen species and decreasing mitochondrial membrane potential. *Toxicol. Vitr.* **2022**, *84*, 105458, doi:10.1016/j.tiv.2022.105458.
37. Kwak, S.W.; Park, E.S.; Lee, C.S. Parthenolide induces apoptosis by activating the mitochondrial and death receptor pathways and inhibits FAK-mediated cell invasion. *Mol. Cell. Biochem.* **2014**, *385*, 133–144, doi:10.1007/s11010-013-1822-4.
38. Wang, H.; Ding, Q.; zhou, H.; Huang, C.; Liu, G.; Zhao, X.; Cheng, Z.; You, X. Dihydroartemisinin inhibited vasculogenic mimicry in gastric cancer through the FGF2/FGFR1 signaling pathway. *Phytomedicine* **2024**, *134*, 155962, doi:https://doi.org/10.1016/j.phymed.2024.155962.
39. Neganova, M.E.; Aleksandrova, Y.R.; Sharova, E. V; Smirnova, E. V; Artyushin, O.I.; Nikolaeva, N.S.; Semakov, A. V; Schagina, I.A.; Akylbekov, N.; Kurmanbayev, R.; et al. Conjugates of 3,5-Bis(arylidene)-4-piperidone and Sesquiterpene Lactones Have an Antitumor Effect via Resetting the Metabolic Phenotype of Cancer Cells. *Molecules* **2024**, *29*, 2765, doi:10.3390/molecules29122765.
40. Ma, X.; Wu, K.; Xu, A.; Jiao, P.; Li, H.; Xing, L. The sesquiterpene lactone eupatolide induces apoptosis in non-small cell lung cancer cells by suppressing STAT3 signaling. *Environ. Toxicol. Pharmacol.* **2021**, *81*, 103513, doi:https://doi.org/10.1016/j.etap.2020.103513.
41. Qu, Z.; Lin, Y.; Mok, D.K.-W.; Bian, Q.; Tai, W.C.-S.; Chen, S. Brevilin A, a Natural Sesquiterpene Lactone Inhibited the Growth of Triple-Negative Breast Cancer Cells via Akt/mTOR and STAT3 Signaling Pathways. *Onco. Targets. Ther.* **2020**, *13*, 5363–5373, doi:10.2147/OTT.S256833.
42. Zhu, Z.; Xu, X.; Shen, C.; Yuan, J.; Lou, S.; Ma, X.; Chen, X.; Yang, B.; Zhao, H. A novel sesquiterpene lactone fraction from Eupatorium chinense L. suppresses hepatocellular carcinoma growth by triggering

ferritinophagy and mitochondrial damage. *Phytomedicine* **2023**, *112*, 154671, doi:https://doi.org/10.1016/j.phymed.2023.154671.

43. Mahalingam, D.; Wilding, G.; Denmeade, S.; Sarantopoulas, J.; Cosgrove, D.; Cetnar, J.; Azad, N.; Bruce, J.; Kurman, M.; Allgood, V.E.; et al. Mipsagargin, a novel thapsigargin-based PSMA-activated prodrug: results of a first-in-man phase I clinical trial in patients with refractory, advanced or metastatic solid tumours. *Br. J. Cancer* **2016**, *114*, 986–994, doi:10.1038/bjc.2016.72.
44. Trimble, C.L.; Levinson, K.; Maldonado, L.; Donovan, M.J.; Clark, K.T.; Fu, J.; Shay, M.E.; Sauter, M.E.; Sanders, S.A.; Frantz, P.S.; et al. A first-in-human proof-of-concept trial of intravaginal artesunate to treat cervical intraepithelial neoplasia 2/3 (CIN2/3). *Gynecol. Oncol.* **2020**, *157*, 188–194, doi:https://doi.org/10.1016/j.ygyno.2019.12.035.
45. Dai, Z.; Li, S.-R.; Zhu, P.-F.; Liu, L.; Wang, B.; Liu, Y.-P.; Luo, X.-D.; Zhao, X.-D. Isocostunolide inhibited glioma stem cell by suppression proliferation and inducing caspase dependent apoptosis. *Bioorg. Med. Chem. Lett.* **2017**, *27*, 2863–2867, doi:10.1016/j.bmcl.2017.04.075.
46. Tang, T.K.; Chiu, S.C.; Lin, C.W.; Su, M.J.; Liao, M.H. Induction of survivin inhibition, G 2 /M cell cycle arrest and autophagic on cell death in human malignant glioblastoma cells. *Chin. J. Physiol.* **2015**, *58*, 95–103, doi:10.4077/CJP.2015.BAC267.
47. Ding, Y.; Xue, Q.; Liu, S.; Hu, K.; Wang, D.; Wang, T.; Li, Y.; Guo, H.; Hao, X.; Ge, W.; et al. Identification of Parthenolide Dimers as Activators of Pyruvate Kinase M2 in Xenografts of Glioblastoma Multiforme in Vivo. *J. Med. Chem.* **2020**, *63*, 1597–1611, doi:10.1021/acs.jmedchem.9b01328.
48. Zhang, Y.J.; Yang, D.L.; Qin, H.X.; He, L.J.; Huang, J.H.; Tang, D.Y.; Xu, Z.G.; Chen, Z.Z.; Li, Y. DMAPT-D6 induces death-receptor-mediated apoptosis to inhibit glioblastoma cell oncogenesis via induction of DNA damage through accumulation of intracellular ROS. *Oncol. Rep.* **2021**, *45*, 1261–1272, doi:10.3892/or.2021.7932.
49. Jia, X.; Liu, Q.; Wang, S.; Zeng, B.; Du, G.; Zhang, C.; Li, Y. Synthesis, cytotoxicity, and in vivo antitumor activity study of parthenolide semicarbazones and thiosemicarbazones. *Bioorg. Med. Chem.* **2020**, *28*, 115557, doi:10.1016/j.bmc.2020.115557.
50. Yan, Q.-L.; Wang, X.-Y.; Bai, M.; Zhang, X.; Song, S.-J.; Yao, G.-D. Sesquiterpene lactones from Elephantopus scaber exhibit cytotoxic effects on glioma cells by targeting GSTP1. *Bioorg. Chem.* **2022**, *129*, 106183, doi:10.1016/j.bioorg.2022.106183.
51. Ahmad, F.; Dixit, D.; Sharma, V.; Kumar, A.; Joshi, S.D.; Sarkar, C.; Sen, E. Nrf2-driven TERT regulates pentose phosphate pathway in glioblastoma. *Cell Death Dis.* **2016**, *7*, e2213, doi:10.1038/cddis.2016.117.
52. Ling, Z.; Pan, J.; Zhang, Z.; Chen, G.; Geng, J.; Lin, Q.; Zhang, T.; Cao, S.; Chen, C.; Lin, J.; et al. Small-molecule Molephantin induces apoptosis and mitophagy flux blockage through ROS production in glioblastoma. *Cancer Lett.* **2024**, *592*, 216927, doi:10.1016/j.canlet.2024.216927.
53. Feng, D.; Liu, M.; Liu, Y.; Zhao, X.; Sun, H.; Zheng, X.; Zhu, J.; Shang, F. Micheliolide suppresses the viability, migration and invasion of U251MG cells via the NF-κB signaling pathway. *Oncol. Lett.* **2020**, *20*, 67, doi:10.3892/ol.2020.11928.
54. An, Y.; Guo, W.; Li, L.; Xu, C.; Yang, D.; Wang, S.; Lu, Y.; Zhang, Q.; Zhai, J.; Fan, H.; et al. Micheliolide derivative DMAMCL inhibits glioma cell growth in vitro and in vivo. *PLoS One* **2015**, *10*, e0116202, doi:10.1371/journal.pone.0116202.
55. Li, Y.; Ni, K.; Chan, C.; Guo, N.; Luo, T.; Han, W.; Culbert, A.; Weichselbaum, R.R.; Lin, W. Dimethylaminomicheliolide Sensitizes Cancer Cells to Radiotherapy for Synergistic Combination with Immune Checkpoint Blockade. *Adv. Ther.* **2022**, *5*, 2100160, doi:10.1002/adtp.202100160.
56. Xi, X.; Liu, N.; Wang, Q.; Chu, Y.; Yin, Z.; Ding, Y.; Lu, Y. ACT001, a novel PAI-1 inhibitor, exerts synergistic effects in combination with cisplatin by inhibiting PI3K/AKT pathway in glioma. *Cell Death Dis.* **2019**, *10*, 757, doi:10.1038/s41419-019-1986-2.
57. Li, Q.; Sun, Y.; Liu, B.; Li, J.; Hao, X.; Ge, W.; Zhang, X.; Bao, S.; Gong, J.; Jiang, Z.; et al. ACT001 modulates the NF-κB/MnSOD/ROS axis by targeting IKKβ to inhibit glioblastoma cell growth. *J. Mol. Med.* **2020**, *98*, 263–277, doi:10.1007/s00109-019-01839-0.
58. Du, Q.-Q.; Tang, M.; Huang, L.-L.; Zhao, R.; Yan, C.; Li, Y.; Pan, X.-D. The antitumor activity and mechanism of MCL3 in G422 glioblastoma. *World J. Tradit. Chinese Med.* **2020**, *6*, 353, doi:10.4103/wjtcm.wjtcm_46_20.
59. Wang, J.; Li, M.; Cui, X.; Lv, D.; Jin, L.; Khan, M.; Ma, T. Brevilin A promotes oxidative stress and induces mitochondrial apoptosis in U87 glioblastoma cells. *Onco. Targets. Ther.* **2018**, *11*, 7031–7040, doi:10.2147/OTT.S179730.
60. Ma, Y.-Y.; Di, Z.-M.; Cao, Q.; Xu, W.-S.; Bi, S.-X.; Yu, J.-S.; Shen, Y.-J.; Yu, Y.-Q.; Shen, Y.-X.; Feng, L.-J. Xanthatin induces glioma cell apoptosis and inhibits tumor growth via activating endoplasmic reticulum stress-dependent CHOP pathway. *Acta Pharmacol. Sin.* **2020**, *41*, 404–414, doi:10.1038/s41401-019-0318-5.
61. Chen, H.; Zhu, T.; Huang, X.; Xu, W.; Di, Z.; Ma, Y.; Xue, M.; Bi, S.; Shen, Y.; Yu, Y.; et al. Xanthatin suppresses proliferation and tumorigenicity of glioma cells through autophagy inhibition via activation of the PI3K-Akt–mTOR pathway. *Pharmacol. Res. Perspect.* **2023**, *11*, 1–13, doi:10.1002/prp2.1041.

62. Ayan, Ç.İ.; Güçlü, E.; Dursun, H.G.; Vural, H. Tomentosin shows anticancer effect on U87 human glioblastoma multiforme cells. *Bull. Biotechnol.* **2021**, *2*, 23–26, doi:10.51539/biotech.1027492.
63. Rotondo, R.; Oliva, M.A.; Arcella, A. The Sesquiterpene Lactone Cynaropicrin Manifests Strong Cytotoxicity in Glioblastoma Cells U-87 MG by Induction of Oxidative Stress. *Biomedicines* **2022**, *10*, doi:10.3390/biomedicines10071583.
64. Zeng, B.; Cheng, Y.; Zheng, K.; Liu, S.; Shen, L.; Hu, J.; Li, Y.; Pan, X. Design, synthesis and in vivo anticancer activity of novel parthenolide and micheliolide derivatives as NF-κB and STAT3 inhibitors. *Bioorg. Chem.* **2021**, *111*, 104973, doi:10.1016/j.bioorg.2021.104973.
65. Wang, X.; Yu, Z.; Wang, C.; Cheng, W.; Tian, X.; Huo, X.; Wang, Y.; Sun, C.; Feng, L.; Xing, J.; et al. Alantolactone, a natural sesquiterpene lactone, has potent antitumor activity against glioblastoma by targeting IKKβ kinase activity and interrupting NF-κB/COX-2-mediated signaling cascades. *J. Exp. Clin. Cancer Res.* **2017**, *36*, 1–14, doi:10.1186/s13046-017-0563-8.
66. Wang, X.; Zou, S.; Ren, T.; Zhao, L.-J.; Yu, L.-F.; Li, X.-Y.; Yan, X.; Zhang, L.-J. Alantolactone suppresses the metastatic phenotype and induces the apoptosis of glioblastoma cells by targeting LIMK kinase activity and activating the cofilin/G-actin signaling cascade. *Int. J. Mol. Med.* **2021**, *47*, 68, doi:10.3892/ijmm.2021.4901.
67. Cao, L.; Duanmu, W.; Yin, Y.; Zhou, Z.; Ge, H.; Chen, T.; Tan, L.; Yu, A.; Hu, R.; Fei, L.; et al. Dihydroartemisinin exhibits anti-glioma stem cell activity through inhibiting p-AKT and activating caspase-3. *Pharmazie* **2014**, *69*, 752–758.
68. Zhang, W.; Wang, Y.; Chen, L.; Chen, H.; Qi, H.; Zheng, Y.; Du, Y.; Zhang, L.; Wang, T.; Li, Q. Dihydroartemisinin suppresses glioma growth by repressing ERRα-mediated mitochondrial biogenesis. *Mol. Cell. Biochem.* **2024**, *479*, 2809–2825, doi:10.1007/s11010-023-04892-z.
69. Beltzig, L.; Christmann, M.; Kaina, B. Abrogation of Cellular Senescence Induced by Temozolomide in Glioblastoma Cells: Search for Senolytics. *Cells* **2022**, *11*, 2588, doi:10.3390/cells11162588.
70. Izumi, C.; Laure, H.J.; Barbosa, N.G.; Thomé, C.H.; Ferreira, G.A.; Sousa, J.P.B.; Lopes, N.P.; Rosa, J.C. Sequesterpene Lactones Isolated from a Brazilian Cerrado Plant (Eremanthus spp.) as Anti-Proliferative Compounds, Characterized by Functional and Proteomic Analysis, are Candidates for New Therapeutics in Glioblastoma. *Int. J. Mol. Sci.* **2020**, *21*, 4713, doi:10.3390/ijms21134713.
71. Lan, C.-W.; Chen, H.-H.; Sheu, J.J.-C. Deoxyelephantopin induces apoptosis and cell cycle arrest in GL261 glioblastoma cells. *Naunyn. Schmiedebergs. Arch. Pharmacol.* **2024**, doi:10.1007/s00210-024-03429-5.
72. Trifunović, S.; Isaković, A.M.; Isaković, A.; Vučković, I.; Mandić, B.; Novaković, M.; Vajs, V.; Milosavljević, S.; Trajković, V. Isolation, characterization, and in vitro cytotoxicity of new sesquiterpenoids from Achillea clavennae. *Planta Med.* **2014**, *80*, 297–305, doi:10.1055/s-0033-1360312.
73. Miklossy, G.; Youn, U.J.; Yue, P.; Zhang, M.; Chen, C.-H.; Hilliard, T.S.; Paladino, D.; Li, Y.; Choi, J.; Sarkaria, J.N.; et al. Hirsutinolide Series Inhibit Stat3 Activity, Alter GCN1, MAP1B, Hsp105, G6PD, Vimentin, TrxR1, and Importin α-2 Expression, and Induce Antitumor Effects against Human Glioma. *J. Med. Chem.* **2015**, *58*, 7734–7748, doi:10.1021/acs.jmedchem.5b00686.
74. Tsujimoto, Y. Cell death regulation by the Bcl-2 protein family in the mitochondria. *J. Cell. Physiol.* **2003**, *195*, 158–167, doi:https://doi.org/10.1002/jcp.10254.
75. Zhang, Y.; Dube, C.; Gibert, M.; Cruickshanks, N.; Wang, B.; Coughlan, M.; Yang, Y.; Setiady, I.; Deveau, C.; Saoud, K.; et al. The p53 Pathway in Glioblastoma. *Cancers (Basel).* **2018**, *10*, 297, doi:10.3390/cancers10090297.
76. Que, Z.; Wang, P.; Hu, Y.; Xue, Y.; Liu, X.; Qu, C.; Ma, J.; Liu, Y. Dihydroartemisin inhibits glioma invasiveness via a ROS to P53 to β-catenin signaling. *Pharmacol. Res.* **2017**, *119*, 72–88, doi:10.1016/j.phrs.2017.01.014.
77. Sun, X.; Dyson, H.J.; Wright, P.E. A phosphorylation-dependent switch in the disordered p53 transactivation domain regulates DNA binding. *Proc. Natl. Acad. Sci.* **2021**, *118*, e2021456118, doi:10.1073/pnas.2021456118.
78. Fung, T.S.; Chakrabarti, R.; Higgs, H.N. The multiple links between actin and mitochondria. *Nat. Rev. Mol. Cell Biol.* **2023**, *24*, 651–667, doi:10.1038/s41580-023-00613-y.
79. Namme, J.N.; Bepari, A.K.; Takebayashi, H. Cofilin Signaling in the CNS Physiology and Neurodegeneration. *Int. J. Mol. Sci.* **2021**, *22*, 10727, doi:10.3390/ijms221910727.
80. Xu, J.; Huang, Y.; Zhao, J.; Wu, L.; Qi, Q.; Liu, Y.; Li, G.; Li, J.; Liu, H.; Wu, H. Cofilin: A Promising Protein Implicated in Cancer Metastasis and Apoptosis. *Front. Cell Dev. Biol.* **2021**, *9*, 599065, doi:10.3389/fcell.2021.599065.
81. Penthala, N.R.; Janganati, V.; Alpe, T.L.; Apana, S.M.; Berridge, M.S.; Crooks, P.A.; Borrelli, M.J. N-[(11)CH(3)]Dimethylaminoparthenolide (DMAPT) uptake into orthotopic 9LSF glioblastoma tumors in the rat. *Bioorg. Med. Chem. Lett.* **2016**, *26*, 5883–5886, doi:10.1016/j.bmcl.2016.11.015.
82. Hexum, J.K.; Becker, C.M.; Kempema, A.M.; Ohlfest, J.R.; Largaespada, D.A.; Harki, D.A. Parthenolide prodrug LC-1 slows growth of intracranial glioma. *Bioorg. Med. Chem. Lett.* **2015**, *25*, 2493–2495, doi:10.1016/j.bmcl.2015.04.058.

83. Dissanayake, A.A.; Bejcek, B.E.; Zhang, C.-R.; Nair, M.G. Sesquiterpenoid Lactones in Tanacetum huronense Inhibit Human Glioblastoma Cell Proliferation. *Nat. Prod. Commun.* **2016**, *11*, 579–582.
84. Janganati, V.; Ponder, J.; Jordan, C.T.; Borrelli, M.J.; Penthala, N.R.; Crooks, P.A. Dimers of Melampomagnolide B Exhibit Potent Anticancer Activity against Hematological and Solid Tumor Cells. *J. Med. Chem.* **2015**, *58*, 8896–8906, doi:10.1021/acs.jmedchem.5b01187.
85. Yang, Z.-J.; Ge, W.-Z.; Li, Q.-Y.; Lu, Y.; Gong, J.-M.; Kuang, B.-J.; Xi, X.; Wu, H.; Zhang, Q.; Chen, Y. Syntheses and Biological Evaluation of Costunolide, Parthenolide, and Their Fluorinated Analogues. *J. Med. Chem.* **2015**, *58*, 7007–7020, doi:10.1021/acs.jmedchem.5b00915.
86. Yan, B.; Zhang, M.M.; Chen, X.; Li, Y.; Khan, M.; Ma, T. Alantolactone Suppresses YAP Signaling and Stemness Properties in Glioblastoma Cells. *Pak. J. Zool.* **2023**, *55*, doi:10.17582/journal.pjz/20230412050411.
87. Hegazy, M.-E.F.; Dawood, M.; Mahmoud, N.; Elbadawi, M.; Sugimoto, Y.; Klauck, S.M.; Mohamed, N.; Efferth, T. 2α-Hydroxyalantolactone from Pulicaria undulata: activity against multidrug-resistant tumor cells and modes of action. *Phytomedicine* **2021**, *81*, 153409, doi:10.1016/j.phymed.2020.153409.
88. Araki, K.; Hara, M.; Hamada, S.; Matsumoto, T.; Nakamura, S. Antiproliferative Activities of Cynaropicrin and Related Compounds against Cancer Stem Cells. *Chem. Pharm. Bull. (Tokyo).* **2024**, *72*, 200–208, doi:10.1248/cpb.c23-00811.
89. Salin, A. V; Shabanov, A.A.; Khayarov, K.R.; Islamov, D.R.; Voloshina, A.D.; Amerhanova, S.K.; Lyubina, A.P. Phosphine-Catalyzed Synthesis and Cytotoxic Evaluation of Michael Adducts of the Sesquiterpene Lactone Arglabin. *ChemMedChem* **2024**, *19*, e202400045, doi:10.1002/cmdc.202400045.
90. Chen, J.; Chen, X.; Wang, F.; Gao, H.; Hu, W. Dihydroartemisinin suppresses glioma proliferation and invasion via inhibition of the ADAM17 pathway. *Neurol. Sci.* **2015**, *36*, 435–440, doi:10.1007/s10072-014-1963-6.
91. Lemke, D.; Pledl, H.-W.; Zorn, M.; Jugold, M.; Green, E.; Blaes, J.; Löw, S.; Hertenstein, A.; Ott, M.; Sahm, F.; et al. Slowing down glioblastoma progression in mice by running or the anti-malarial drug dihydroartemisinin? Induction of oxidative stress in murine glioblastoma therapy. *Oncotarget* **2016**, *7*, 56713–56725, doi:10.18632/oncotarget.10723.
92. Chen, J.; Hu, J.; Li, X.; Zong, S.; Zhang, G.; Guo, Z.; Jing, Z. Enhydrin suppresses the malignant phenotype of GBM via Jun/Smad7/TGF-β1 signaling pathway. *Biochem. Pharmacol.* **2024**, *226*, 116380, doi:10.1016/j.bcp.2024.116380.
93. Ježek, J.; Cooper, K.; Strich, R. Reactive Oxygen Species and Mitochondrial Dynamics: The Yin and Yang of Mitochondrial Dysfunction and Cancer Progression. *Antioxidants* **2018**, *7*, 13, doi:10.3390/antiox7010013.
94. He, F.; Ru, X.; Wen, T. NRF2, a Transcription Factor for Stress Response and Beyond. *Int. J. Mol. Sci.* **2020**, *21*, 4777, doi:10.3390/ijms21134777.
95. Hong, Y.; Boiti, A.; Vallone, D.; Foulkes, N.S. Reactive Oxygen Species Signaling and Oxidative Stress: Transcriptional Regulation and Evolution. *Antioxidants* **2024**, *13*, 312, doi:10.3390/antiox13030312.
96. Agrawal, K.; Asthana, S.; Kumar, D. Role of Oxidative Stress in Metabolic Reprogramming of Brain Cancer. *Cancers (Basel).* **2023**, *15*, 4920, doi:10.3390/cancers15204920.
97. Salazar-Ramiro, A.; Ramírez-Ortega, D.; Pérez de la Cruz, V.; Hérnandez-Pedro, N.Y.; González-Esquivel, D.F.; Sotelo, J.; Pineda, B. Role of Redox Status in Development of Glioblastoma. *Front. Immunol.* **2016**, *7*, 156, doi:10.3389/fimmu.2016.00156.
98. Zhang, Z.; Qiao, Y.; Sun, Q.; Peng, L.; Sun, L. A novel SLC25A1 inhibitor, parthenolide, suppresses the growth and stemness of liver cancer stem cells with metabolic vulnerability. *Cell Death Discov.* **2023**, *9*, 350, doi:10.1038/s41420-023-01640-6.
99. Gao, J.; Zhao, Y.; Li, T.; Gan, X.; Yu, H. The Role of PKM2 in the Regulation of Mitochondrial Function: Focus on Mitochondrial Metabolism, Oxidative Stress, Dynamic, and Apoptosis. PKM2 in Mitochondrial Function. *Oxid. Med. Cell. Longev.* **2022**, *2022*, 7702681, doi:https://doi.org/10.1155/2022/7702681.
100. Kumari, R.; Jat, P. Mechanisms of Cellular Senescence: Cell Cycle Arrest and Senescence Associated Secretory Phenotype. *Front. Cell Dev. Biol.* **2021**, *9*, 645593, doi:10.3389/fcell.2021.645593.
101. Valieva, Y.; Ivanova, E.; Fayzullin, A.; Kurkov, A.; Igrunkova, A. Senescence-Associated β-Galactosidase Detection in Pathology. *Diagnostics* **2022**, *12*, 2309, doi:10.3390/diagnostics12102309.
102. Chojak, R.; Fares, J.; Petrosyan, E.; Lesniak, M.S. Cellular senescence in glioma. *J. Neurooncol.* **2023**, *164*, 11–29, doi:10.1007/s11060-023-04387-3.
103. Salam, R.; Saliou, A.; Bielle, F.; Bertrand, M.; Antoniewski, C.; Carpentier, C.; Alentorn, A.; Capelle, L.; Sanson, M.; Huillard, E.; et al. Cellular senescence in malignant cells promotes tumor progression in mouse and patient Glioblastoma. *Nat. Commun.* **2023**, *14*, 441, doi:10.1038/s41467-023-36124-9.
104. Høyer-Hansen, M.; Jäättelä, M. Connecting endoplasmic reticulum stress to autophagy by unfolded protein response and calcium. *Cell Death Differ.* **2007**, *14*, 1576–1582, doi:10.1038/sj.cdd.4402200.
105. Shi, P.; Zhang, Z.; Xu, J.; Zhang, L.; Cui, H. Endoplasmic reticulum stress-induced cell death as a potential mechanism for targeted therapy in glioblastoma (Review). *Int J Oncol* **2021**, *59*, 60, doi:10.3892/ijo.2021.5240.

106. Khabibov, M.; Garifullin, A.; Boumber, Y.; Khaddour, K.; Fernandez, M.; Khamitov, F.; Khalikova, L.; Kuznetsova, N.; Kit, O.; Kharin, L. Signaling pathways and therapeutic approaches in glioblastoma multiforme (Review). *Int. J. Oncol.* **2022**, *60*, 69, doi:10.3892/ijo.2022.5359.
107. Abbott, N.J.; Patabendige, A.A.K.; Dolman, D.E.M.; Yusof, S.R.; Begley, D.J. Structure and function of the blood-brain barrier. *Neurobiol. Dis.* 2010, *37*.
108. Bors, L.A.; Erdö, F. Overcoming the blood-brain barrier. Challenges and tricks for CNS drug delivery. *Sci. Pharm.* 2019, *87*.
109. Velumani, K.; John, A.; Shaik, M.R.; Hussain, S.A.; Guru, A.; Issac, P.K. Exploring sesquiterpene lactone as a dual therapeutic agent for diabetes and oxidative stress: insights into PI3K/AKT modulation. *3 Biotech* **2024**, *14*, 205, doi:10.1007/s13205-024-04050-2.
110. Khalil, M.N.A.; Choucry, M.A.; El Senousy, A.S.; Hassan, A.; El-Marasy, S.A.; El Awdan, S.A.; Omar, F.A. Ambrosin, a potent NF-κβ inhibitor, ameliorates lipopolysaccharide induced memory impairment, comparison to curcumin. *PLoS One* **2019**, *14*, doi:10.1371/journal.pone.0219378.
111. Verma, S.S.; Rai, V.; Awasthee, N.; Dhasmana, A.; Rajalaksmi, D.S.; Nair, M.S.; Gupta, S.C. Isodeoxyelephantopin, a Sesquiterpene Lactone Induces ROS Generation, Suppresses NF-κB Activation, Modulates LncRNA Expression and Exhibit Activities Against Breast Cancer. *Sci. Rep.* **2019**, *9*, 1–16, doi:10.1038/s41598-019-52971-3.
112. Ávila-Gálvez, M.Á.; Marques, D.; Figueira, I.; Cankar, K.; Bosch, D.; Brito, M.A.; dos Santos, C.N. Costunolide and parthenolide: Novel blood-brain barrier permeable sesquiterpene lactones to improve barrier tightness. *Biomed. Pharmacother.* **2023**, *167*, 115413, doi:https://doi.org/10.1016/j.biopha.2023.115413.
113. Tang, J.J.; Huang, L.F.; Deng, J. Le; Wang, Y.M.; Guo, C.; Peng, X.N.; Liu, Z.; Gao, J.M. Cognitive enhancement and neuroprotective effects of OABL, a sesquiterpene lactone in 5xFAD Alzheimer's disease mice model. *Redox Biol.* **2022**, *50*, 102229, doi:10.1016/j.redox.2022.102229.
114. Rummel, C.; Gerstberger, R.; Roth, J.; Hübschle, T. Parthenolide attenuates LPS-induced fever, circulating cytokines and markers of brain inflammation in rats. *Cytokine* **2011**, *56*, doi:10.1016/j.cyto.2011.09.022.
115. Wang, X.; Lan, Y.L.; Xing, J.S.; Lan, X.Q.; Wang, L.T.; Zhang, B. Alantolactone plays neuroprotective roles in traumatic brain injury in rats via anti-inflammatory, anti-oxidative and anti-apoptosis pathways. *Am. J. Transl. Res.* **2018**, *10*.
116. Xu, C.; Hou, P.; Li, X.; Xiao, M.; Zhang, Z.; Li, Z.; Xu, J.; Liu, G.; Tan, Y.; Fang, C. Comprehensive understanding of glioblastoma molecular phenotypes: classification, characteristics, and transition. *Cancer Biol. Med.* **2024**, *21*, 363–381, doi:10.20892/j.issn.2095-3941.2023.0510.
117. Xu, D.; Wu, H.; Tian, M.; Liu, Q.; Zhu, Y.; Zhang, H.; Zhang, X.; Shen, H. Isolinderalactone suppresses pancreatic ductal adenocarcinoma by activating p38 MAPK to promote DDIT3 expression and trigger endoplasmic reticulum stress. *Int. Immunopharmacol.* **2024**, *143*, 113497, doi:10.1016/j.intimp.2024.113497.
118. Tian, Y.; Ma, B.; Zhao, X.; Tian, S.; Li, Y.; Pei, H.; Yu, S.; Liu, C.; Lin, Z.; Zuo, Z.; et al. Dehydrocostus lactone inhibits the proliferation and metastasis of hepatocellular carcinoma cells via modulating p53-p21-CDK2 signaling pathway. *Arab. J. Chem.* **2023**, *16*, 104994, doi:https://doi.org/10.1016/j.arabjc.2023.104994.
119. Zhu, S.M.; Park, Y.R.; Seo, S.Y.; Kim, I.H.; Lee, S.T.; Kim, S.W. Parthenolide inhibits transforming growth factor β1-induced epithelial-mesenchymal transition in colorectal cancer cells. *Intest. Res.* **2019**, *17*, 527–536, doi:10.5217/ir.2019.00031.
120. Wang, Z.; Shi, Y.; Ying, C.; Jiang, Y.; Hu, J. Hypoxia-induced PLOD1 overexpression contributes to the malignant phenotype of glioblastoma via NF-κB signaling. *Oncogene* **2021**, *40*, 1458–1475, doi:10.1038/s41388-020-01635-y.
121. Qiu, W.; Song, S.; Chen, W.; Zhang, J.; Yang, H.; Chen, Y. Hypoxia-induced EPHB2 promotes invasive potential of glioblastoma. *Int. J. Clin. Exp. Pathol.* **2019**, *12*, 539–548.
122. Yee, P.P.; Wei, Y.; Kim, S.-Y.; Lu, T.; Chih, S.Y.; Lawson, C.; Tang, M.; Liu, Z.; Anderson, B.; Thamburaj, K.; et al. Neutrophil-induced ferroptosis promotes tumor necrosis in glioblastoma progression. *Nat. Commun.* **2020**, *11*, 5424, doi:10.1038/s41467-020-19193-y.
123. Kesanakurti, D.; Maddirela, D.; Banasavadi-Siddegowda, Y.K.; Lai, T.-H.; Qamri, Z.; Jacob, N.K.; Sampath, D.; Mohanam, S.; Kaur, B.; Puduvalli, V.K. A novel interaction of PAK4 with PPARγ to regulate Nox1 and radiation-induced epithelial-to-mesenchymal transition in glioma. *Oncogene* **2017**, *36*, 5309–5320, doi:10.1038/onc.2016.261.
124. Yoo, K.-C.; Kang, J.-H.; Choi, M.-Y.; Suh, Y.; Zhao, Y.; Kim, M.-J.; Chang, J.H.; Shim, J.-K.; Yoon, S.-J.; Kang, S.-G.; et al. Soluble ICAM-1 a Pivotal Communicator between Tumors and Macrophages, Promotes Mesenchymal Shift of Glioblastoma. *Adv. Sci. (Weinheim, Baden-Wurttemberg, Ger.* **2022**, *9*, e2102768, doi:10.1002/advs.202102768.
125. Liu, Z.; Kuang, W.; Zhou, Q.; Zhang, Y. TGF-β1 secreted by M2 phenotype macrophages enhances the stemness and migration of glioma cells via the SMAD2/3 signalling pathway. *Int J Mol Med* **2018**, *42*, 3395–3403, doi:10.3892/ijmm.2018.3923.

126. Oliveira, M.N.; Pillat, M.M.; Motaln, H.; Ulrich, H.; Lah, T.T. Kinin-B1 Receptor Stimulation Promotes Invasion and is Involved in Cell-Cell Interaction of Co-Cultured Glioblastoma and Mesenchymal Stem Cells. *Sci. Rep.* **2018**, *8*, 1299, doi:10.1038/s41598-018-19359-1.
127. Lim, E.-J.; Kim, S.; Oh, Y.; Suh, Y.; Kaushik, N.; Lee, J.-H.; Lee, H.-J.; Kim, M.-J.; Park, M.-J.; Kim, R.-K.; et al. Crosstalk between GBM cells and mesenchymal stemlike cells promotes the invasiveness of GBM through the C5a/p38/ZEB1 axis. *Neuro. Oncol.* **2020**, *22*, 1452–1462, doi:10.1093/neuonc/noaa064.
128. Yan, T.; Tan, Y.; Deng, G.; Sun, Z.; Liu, B.; Wang, Y.; Yuan, F.; Sun, Q.; Hu, P.; Gao, L.; et al. TGF-β induces GBM mesenchymal transition through upregulation of CLDN4 and nuclear translocation to activate TNF-α/NF-κB signal pathway. *Cell Death Dis.* **2022**, *13*, 339, doi:10.1038/s41419-022-04788-8.
129. Wu, J.; Shen, S.; Liu, T.; Ren, X.; Zhu, C.; Liang, Q.; Cui, X.; Chen, L.; Cheng, P.; Cheng, W.; et al. Chemerin enhances mesenchymal features of glioblastoma by establishing autocrine and paracrine networks in a CMKLR1-dependent manner. *Oncogene* **2022**, *41*, 3024–3036, doi:10.1038/s41388-022-02295-w.
130. Alafate, W.; Li, X.; Zuo, J.; Zhang, H.; Xiang, J.; Wu, W.; Xie, W.; Bai, X.; Wang, M.; Wang, J. Elevation of CXCL1 indicates poor prognosis and radioresistance by inducing mesenchymal transition in glioblastoma. *CNS Neurosci. Ther.* **2020**, *26*, 475–485, doi:10.1111/cns.13297.
131. Neftel, C.; Laffy, J.; Filbin, M.G.; Hara, T.; Shore, M.E.; Rahme, G.J.; Richman, A.R.; Silverbush, D.; Shaw, M.L.; Hebert, C.M.; et al. An Integrative Model of Cellular States, Plasticity, and Genetics for Glioblastoma. *Cell* **2019**, *178*, 835-849.e21, doi:https://doi.org/10.1016/j.cell.2019.06.024.
132. Pastushenko, I.; Blanpain, C. EMT Transition States during Tumor Progression and Metastasis. *Trends Cell Biol.* **2019**, *29*, 212–226, doi:10.1016/j.tcb.2018.12.001.
133. Yamini, B. NF-κB, Mesenchymal Differentiation and Glioblastoma. *Cells* 2018, *7*, 125.
134. Li, G.; Li, Y.; Liu, X.; Wang, Z.; Zhang, C.; Wu, F.; Jiang, H.; Zhang, W.; Bao, Z.; Wang, Y.; et al. ALDH1A3 induces mesenchymal differentiation and serves as a predictor for survival in glioblastoma. *Cell Death Dis.* **2018**, *9*, 1190, doi:10.1038/s41419-018-1232-3.
135. Liang, Y.; Voshart, D.; Paridaen, J.T.M.L.; Oosterhof, N.; Liang, D.; Thiruvalluvan, A.; Zuhorn, I.S.; den Dunnen, W.F.A.; Zhang, G.; Lin, H.; et al. CD146 increases stemness and aggressiveness in glioblastoma and activates YAP signaling. *Cell. Mol. Life Sci.* **2022**, *79*, 398, doi:10.1007/s00018-022-04420-0.
136. Yin, J.; Oh, Y.T.; Kim, J.-Y.; Kim, S.S.; Choi, E.; Kim, T.H.; Hong, J.H.; Chang, N.; Cho, H.J.; Sa, J.K.; et al. Transglutaminase 2 Inhibition Reverses Mesenchymal Transdifferentiation of Glioma Stem Cells by Regulating C/EBPβ Signaling. *Cancer Res.* **2017**, *77*, 4973–4984, doi:10.1158/0008-5472.CAN-17-0388.
137. Angel, I.; Pilo Kerman, O.; Rousso-Noori, L.; Friedmann-Morvinski, D. Tenascin C promotes cancer cell plasticity in mesenchymal glioblastoma. *Oncogene* **2020**, *39*, 6990–7004, doi:10.1038/s41388-020-01506-6.
138. Yang, W.; Wu, P.-F.; Ma, J.-X.; Liao, M.-J.; Wang, X.-H.; Xu, L.-S.; Xu, M.-H.; Yi, L. Sortilin promotes glioblastoma invasion and mesenchymal transition through GSK-3β/β-catenin/twist pathway. *Cell Death Dis.* **2019**, *10*, 208, doi:10.1038/s41419-019-1449-9.
139. Zhang, C.; Han, X.; Xu, X.; Zhou, Z.; Chen, X.; Tang, Y.; Cheng, J.; Moazzam, N.F.; Liu, F.; Xu, J.; et al. FoxM1 drives ADAM17/EGFR activation loop to promote mesenchymal transition in glioblastoma. *Cell Death Dis.* **2018**, *9*, 469, doi:10.1038/s41419-018-0482-4.
140. Sha, Z.; Zhou, J.; Wu, Y.; Zhang, T.; Li, C.; Meng, Q.; Musunuru, P.P.; You, F.; Wu, Y.; Yu, R.; et al. BYSL Promotes Glioblastoma Cell Migration, Invasion, and Mesenchymal Transition Through the GSK-3β/β-Catenin Signaling Pathway. *Front. Oncol.* **2020**, *10*, 565225, doi:10.3389/fonc.2020.565225.
141. Tao, W.; Chu, C.; Zhou, W.; Huang, Z.; Zhai, K.; Fang, X.; Huang, Q.; Zhang, A.; Wang, X.; Yu, X.; et al. Dual Role of WISP1 in maintaining glioma stem cells and tumor-supportive macrophages in glioblastoma. *Nat. Commun.* **2020**, *11*, 3015, doi:10.1038/s41467-020-16827-z.
142. Jing, D.; Zhang, Q.; Yu, H.; Zhao, Y.; Shen, L. Identification of WISP1 as a novel oncogene in glioblastoma. *Int. J. Oncol.* **2017**, *51*, 1261–1270, doi:10.3892/ijo.2017.4119.
143. Hernández-Vega, A.M.; Del Moral-Morales, A.; Zamora-Sánchez, C.J.; Piña-Medina, A.G.; González-Arenas, A.; Camacho-Arroyo, I. Estradiol Induces Epithelial to Mesenchymal Transition of Human Glioblastoma Cells. *Cells* **2020**, *9*, 1930, doi:10.3390/cells9091930.
144. Khan, A.B.; Lee, S.; Harmanci, A.S.; Patel, R.; Latha, K.; Yang, Y.; Marisetty, A.; Lee, H.-K.; Heimberger, A.B.; Fuller, G.N.; et al. CXCR4 expression is associated with proneural-to-mesenchymal transition in glioblastoma. *Int. J. cancer* **2023**, *152*, 713–724, doi:10.1002/ijc.34329.
145. Xue, B.; Xiang, W.; Zhang, Q.; Wang, H.; Zhou, Y.; Tian, H.; Abdelmaksou, A.; Xue, J.; Sun, M.; Yi, D.; et al. CD90low glioma-associated mesenchymal stromal/stem cells promote temozolomide resistance by activating FOXS1-mediated epithelial-mesenchymal transition in glioma cells. *Stem Cell Res. Ther.* **2021**, *12*, 394, doi:10.1186/s13287-021-02458-8.
146. Lv, S.-Q.; Fu, Z.; Yang, L.; Li, Q.-R.; Zhu, J.; Gai, Q.-J.; Mao, M.; He, J.; Qin, Y.; Yao, X.-X.; et al. Comprehensive omics analyses profile genesets related with tumor heterogeneity of multifocal glioblastomas and reveal LIF/CCL2 as biomarkers for mesenchymal subtype. *Theranostics* **2022**, *12*, 459–473, doi:10.7150/thno.65739.

147. Natesh, K.; Bhosale, D.; Desai, A.; Chandrika, G.; Pujari, R.; Jagtap, J.; Chugh, A.; Ranade, D.; Shastry, P. Oncostatin-M differentially regulates mesenchymal and proneural signature genes in gliomas via STAT3 signaling. *Neoplasia* **2015**, *17*, 225–237, doi:10.1016/j.neo.2015.01.001.
148. Bhat, K.P.L.; Salazar, K.L.; Balasubramaniyan, V.; Wani, K.; Heathcock, L.; Hollingsworth, F.; James, J.D.; Gumin, J.; Diefes, K.L.; Kim, S.H.; et al. The transcriptional coactivator TAZ regulates mesenchymal differentiation in malignant glioma. *Genes Dev.* **2011**, *25*, 2594–2609, doi:10.1101/gad.176800.111.
149. Carro, M.S.; Lim, W.K.; Alvarez, M.J.; Bollo, R.J.; Zhao, X.; Snyder, E.Y.; Sulman, E.P.; Anne, S.L.; Doetsch, F.; Colman, H.; et al. The transcriptional network for mesenchymal transformation of brain tumours. *Nature* **2010**, *463*, 318–325, doi:10.1038/nature08712.
150. Fan, L.; Chen, Z.; Wu, X.; Cai, X.; Feng, S.; Lu, J.; Wang, H.; Liu, N. Ubiquitin-Specific Protease 3 Promotes Glioblastoma Cell Invasion and Epithelial–Mesenchymal Transition via Stabilizing Snail. *Mol. Cancer Res.* **2019**, *17*, 1975–1984, doi:10.1158/1541-7786.MCR-19-0197.
151. Chesnelong, C.; Hao, X.; Cseh, O.; Wang, A.Y.; Luchman, H.A.; Weiss, S. SLUG Directs the Precursor State of Human Brain Tumor Stem Cells. *Cancers (Basel).* **2019**, *11*, 1635, doi:10.3390/cancers11111635.
152. Pölönen, P.; Jawahar Deen, A.; Leinonen, H.M.; Jyrkkänen, H.-K.; Kuosmanen, S.; Mononen, M.; Jain, A.; Tuomainen, T.; Pasonen-Seppänen, S.; Hartikainen, J.M.; et al. Nrf2 and SQSTM1/p62 jointly contribute to mesenchymal transition and invasion in glioblastoma. *Oncogene* **2019**, *38*, 7473–7490, doi:10.1038/s41388-019-0956-6.
153. Cheng, P.; Wang, J.; Waghmare, I.; Sartini, S.; Coviello, V.; Zhang, Z.; Kim, S.-H.; Mohyeldin, A.; Pavlyukov, M.S.; Minata, M.; et al. FOXD1-ALDH1A3 Signaling Is a Determinant for the Self-Renewal and Tumorigenicity of Mesenchymal Glioma Stem Cells. *Cancer Res.* **2016**, *76*, 7219–7230, doi:10.1158/0008-5472.CAN-15-2860.
154. Chong, Y.K.; Sandanaraj, E.; Koh, L.W.H.; Thangaveloo, M.; Tan, M.S.Y.; Koh, G.R.H.; Toh, T.B.; Lim, G.G.Y.; Holbrook, J.D.; Kon, O.L.; et al. ST3GAL1-Associated Transcriptomic Program in Glioblastoma Tumor Growth, Invasion, and Prognosis. *J. Natl. Cancer Inst.* **2016**, *108*, doi:10.1093/jnci/djv326.
155. Chen, Z.; Wang, H.-W.; Wang, S.; Fan, L.; Feng, S.; Cai, X.; Peng, C.; Wu, X.; Lu, J.; Chen, D.; et al. USP9X deubiquitinates ALDH1A3 and maintains mesenchymal identity in glioblastoma stem cells. *J. Clin. Invest.* **2019**, *129*, 2043–2055, doi:10.1172/JCI126414.
156. Qiu, W.; Xiao, Z.; Yang, Y.; Jiang, L.; Song, S.; Qi, X.; Chen, Y.; Yang, H.; Liu, J.; Chu, L. USP10 deubiquitinates RUNX1 and promotes proneural-to-mesenchymal transition in glioblastoma. *Cell Death Dis.* **2023**, *14*, 207, doi:10.1038/s41419-023-05734-y.
157. Zhang, Q.; Chen, Z.; Tang, Q.; Wang, Z.; Lu, J.; You, Y.; Wang, H. USP21 promotes self-renewal and tumorigenicity of mesenchymal glioblastoma stem cells by deubiquitinating and stabilizing FOXD1. *Cell Death Dis.* **2022**, *13*, 712, doi:10.1038/s41419-022-05163-3.
158. Qiu, W.; Cai, X.; Xu, K.; Song, S.; Xiao, Z.; Hou, Y.; Qi, X.; Liu, F.; Chen, Y.; Yang, H.; et al. PRL1 Promotes Glioblastoma Invasion and Tumorigenesis via Activating USP36-Mediated Snail2 Deubiquitination. *Front. Oncol.* **2021**, *11*, 795633, doi:10.3389/fonc.2021.795633.
159. Jiang, Y.-W.; Cheng, H.-Y.; Kuo, C.-L.; Way, T.-D.; Lien, J.-C.; Chueh, F.-S.; Lin, Y.-L.; Chung, J.-G. Tetrandrine inhibits human brain glioblastoma multiforme GBM 8401 cancer cell migration and invasion in vitro. *Environ. Toxicol.* **2019**, *34*, 364–374, doi:https://doi.org/10.1002/tox.22691.
160. Zou, M.; Duan, Y.; Wang, P.; Gao, R.; Chen, X.; Ou, Y.; Liang, M.; Wang, Z.; Yuan, Y.; Wang, L.; et al. DYT-40, a novel synthetic 2-styryl-5-nitroimidazole derivative, blocks malignant glioblastoma growth and invasion by inhibiting AEG-1 and NF-κB signaling pathways. *Sci. Rep.* **2016**, *6*, 27331, doi:10.1038/srep27331.
161. Chen, B.; Li, X.; Wu, L.; Zhou, D.; Song, Y.; Zhang, L.; Wu, Q.; He, Q.; Wang, G.; Liu, X.; et al. Quercetin Suppresses Human Glioblastoma Migration and Invasion via GSK3β/β-catenin/ZEB1 Signaling Pathway. *Front. Pharmacol.* **2022**, *13*.
162. Zhang, X.; Zheng, K.; Li, C.; Zhao, Y.; Li, H.; Liu, X.; Long, Y.; Yao, J. Nobiletin inhibits invasion via inhibiting AKT/GSK3β/β-catenin signaling pathway in Slug-expressing glioma cells. *Oncol. Rep.* **2017**, *37*, doi:10.3892/or.2017.5522.
163. Liu, H.-W.; Su, Y.-K.; Bamodu, O.A.; Hueng, D.-Y.; Lee, W.-H.; Huang, C.-C.; Deng, L.; Hsiao, M.; Chien, M.-H.; Yeh, C.-T.; et al. The Disruption of the β-Catenin/TCF-1/STAT3 Signaling Axis by 4-Acetylantroquinonol B Inhibits the Tumorigenesis and Cancer Stem-Cell-Like Properties of Glioblastoma Cells, In Vitro and In Vivo. *Cancers (Basel).* 2018, *10*, 491.
164. Li, Z.; Zhu, T.; Xu, Y.; Wu, C.; Chen, J.; Ren, Y.; Kong, L.; Sun, S.; Guo, W.; Wang, Y.; et al. A novel STAT3 inhibitor, HJC0152, exerts potent antitumor activity in glioblastoma. *Am. J. Cancer Res.* **2019**, *9*, 699–713.
165. Jia, M.; Wang, Y.; Guo, Y.; Yu, P.; Sun, Y.; Song, Y.; Zhao, L. Nitidine chloride suppresses epithelial-mesenchymal transition and stem cell-like properties in glioblastoma by regulating JAK2/STAT3 signaling. *Cancer Med.* **2021**, *10*, 3113–3128, doi:https://doi.org/10.1002/cam4.3869.

166. Zhang, X.; Wang, X.; Xu, R.; Ji, J.; Xu, Y.; Han, M.; Wei, Y.; Huang, B.; Chen, A.; Zhang, Q.; et al. YM155 decreases radiation-induced invasion and reverses epithelial–mesenchymal transition by targeting STAT3 in glioblastoma. *J. Transl. Med.* **2018**, *16*, 79, doi:10.1186/s12967-018-1451-5.
167. Yang, J.; Antin, P.; Berx, G.; Blanpain, C.; Brabletz, T.; Bronner, M.; Campbell, K.; Cano, A.; Casanova, J.; Christofori, G.; et al. Guidelines and definitions for research on epithelial–mesenchymal transition. *Nat. Rev. Mol. Cell Biol.* **2020**, *21*, 341–352, doi:10.1038/s41580-020-0237-9.
168. Verhaak, R.G.W.; Hoadley, K.A.; Purdom, E.; Wang, V.; Qi, Y.; Wilkerson, M.D.; Miller, C.R.; Ding, L.; Golub, T.; Mesirov, J.P.; et al. Integrated genomic analysis identifies clinically relevant subtypes of glioblastoma characterized by abnormalities in PDGFRA, IDH1, EGFR, and NF1. *Cancer Cell* **2010**, *17*, 98–110, doi:10.1016/j.ccr.2009.12.020.
169. Zhang, T.; Zhang, X.; Lin, C.; Wu, S.; Wang, F.; Wang, H.; Wang, Y.; Peng, Y.; Hutchinson, M.R.; Li, H.; et al. Artemisinin inhibits TLR4 signaling by targeting co-receptor MD2 in microglial BV-2 cells and prevents lipopolysaccharide-induced blood–brain barrier leakage in mice. *J. Neurochem.* **2021**, *157*, doi:10.1111/jnc.15302.
170. Chen, D.; Li, G.; Luo, L.; Lin, T.; Chu, X.; Liu, K.; Lai, T.; Liao, Y.; Lin, X.; Chen, J. Artemisitene induces apoptosis of breast cancer cells by targeting FDFT1 and inhibits the growth of breast cancer patient-derived organoids. *Phytomedicine* **2024**, *135*, 156155, doi:https://doi.org/10.1016/j.phymed.2024.156155.
171. Omotuyi, I.O.; Nash, O.; Metibemu, S.D.; Iwegbulam, G.C.; Olatunji, O.M.; Agbebi, E.; Falade, C.O. Dihydroartemisinin binds human PI3K-β affinity pocket and forces flat conformation in P-loop MET783: A molecular dynamics study. *Comput. Toxicol.* **2023**, *27*, doi:10.1016/j.comtox.2023.100281.
172. Fu, Z.; Li, S.; Liu, J.; Zhang, C.; Jian, C.; Wang, L.; Zhang, Y.; Shi, C. Natural Product Alantolactone Targeting AKR1C1 Suppresses Cell Proliferation and Metastasis in Non-Small-Cell Lung Cancer. *Front. Pharmacol.* **2022**, *13*, doi:10.3389/fphar.2022.847906.
173. Li, J.-K.; Jiang, X.-L.; Zhang, Z.; Chen, W.-Q.; Peng, J.-J.; Liu, B.; Zhu, P.-L.; Yung, K.-K.-L. Isoalantolactone exerts anti-melanoma effects via inhibiting PI3K/AKT/mTOR and STAT3 signaling in cell and mouse models. *Phytother. Res.* **2024**, *38*, 2800–2817, doi:10.1002/ptr.8132.
174. Wang, P.; Yang, H.; Lin, W.; Zhou, J.; Liu, Y.; Ma, L.; Li, M.; Hu, Y.; Yu, C.; Zhang, Y.; et al. Discovery of Novel Sesquiterpene Lactone Derivatives as Potent PKM2 Activators for the Treatment of Ulcerative Colitis. *J. Med. Chem.* **2023**, *66*, doi:10.1021/acs.jmedchem.2c01856.
175. Liu, W.; Yang, W.; Niu, R.; Cong, L.; Jiang, M.; Bai, G. Costunolide covalently targets and inhibits CaMKII phosphorylation to reduce ischemia-associated brain damage. *Phytomedicine* **2023**, *115*, doi:10.1016/j.phymed.2023.154822.
176. Liu, Y.C.; Feng, N.; Li, W.W.; Tu, P.F.; Chen, J.P.; Han, J.Y.; Zeng, K.W. Costunolide Plays an Anti-Neuroinflammation Role in Lipopolysaccharide-Induced BV2 Microglial Activation by Targeting Cyclin-Dependent Kinase 2. *Molecules* **2020**, *25*, doi:10.3390/molecules25122840.
177. Zhuge, W.; Chen, R.; Vladimir, K.; Dong, X.; Zia, K.; Sun, X.; Dai, X.; Bao, M.; Shen, X.; Liang, G. Costunolide specifically binds and inhibits thioredoxin reductase 1 to induce apoptosis in colon cancer. *Cancer Lett.* **2018**, *412*, doi:10.1016/j.canlet.2017.10.006.
178. Yan, Q.L.; Wang, X.Y.; Bai, M.; Zhang, X.; Song, S.J.; Yao, G.D. Sesquiterpene lactones from Elephantopus scaber exhibit cytotoxic effects on glioma cells by targeting GSTP1. *Bioorg. Chem.* **2022**, *129*, doi:10.1016/j.bioorg.2022.106183.
179. Yang, L.; Chen, H.; Hu, Q.; Liu, L.; Yuan, Y.; Zhang, C.; Tang, J.; Shen, X. Eupalinolide B attenuates lipopolysaccharide-induced acute lung injury through inhibition of NF-κB and MAPKs signaling by targeting TAK1 protein. *Int. Immunopharmacol.* **2022**, *111*, doi:10.1016/j.intimp.2022.109148.
180. Li, X.; Kong, L.; Yang, Q.; Duan, A.; Ju, X.; Cai, B.; Chen, L.; An, T.; Li, Y. Parthenolide inhibits ubiquitin-specific peptidase 7 (USP7), Wnt signaling, and colorectal cancer cell growth. *J. Biol. Chem.* **2020**, *295*, doi:10.1074/jbc.RA119.011396.
181. Berdan, C.A.; Ho, R.; Lehtola, H.S.; To, M.; Hu, X.; Huffman, T.R.; Petri, Y.; Altobelli, C.R.; Demeulenaere, S.G.; Olzmann, J.A.; et al. Parthenolide Covalently Targets and Inhibits Focal Adhesion Kinase in Breast Cancer Cells. *Cell Chem. Biol.* **2019**, *26*, doi:10.1016/j.chembiol.2019.03.016.
182. Shin, M.; McGowan, A.; Dinatale, G.J.; Chiramanewong, T.; Cai, T.; Connor, R.E. Hsp72 Is an Intracellular Target of the α,β-Unsaturated Sesquiterpene Lactone, Parthenolide. *ACS Omega* **2017**, *2*, doi:10.1021/acsomega.7b00954.
183. García-Piñeres, A.J.; Lindenmeyer, M.T.; Merfort, I. Role of cysteine residues of p65/NF-κB on the inhibition by the sesquiterpene lactone parthenolide and N-ethyl maleimide, and on its transactivating potential. *Life Sci.* **2004**, *75*, doi:10.1016/j.lfs.2004.01.024.
184. Zhang, S.; Ju, X.; Yang, Q.; Zhu, Y.; Fan, D.; Su, G.; Kong, L.; Li, Y. USP47 maintains the stemness of colorectal cancer cells and is inhibited by parthenolide. *Biochem. Biophys. Res. Commun.* **2021**, *562*, doi:10.1016/j.bbrc.2021.05.017.

185. El Gaafary, M.; Morad, S.A.F.; Schmiech, M.; Syrovets, T.; Simmet, T. Arglabin, an EGFR receptor tyrosine kinase inhibitor, suppresses proliferation and induces apoptosis in prostate cancer cells. *Biomed. Pharmacother.* **2022**, *156*, doi:10.1016/j.biopha.2022.113873.
186. La, C.; Li, M.; Wang, Z.; Liu, T.; Zeng, Q.; Sun, P.; Ren, Z.; Ye, C.; Liu, Q.; Wang, Y. Isolation and anti-neuroinflammation activity of sesquiterpenoids from Artemisia argyi: computational simulation and experimental verification. *BMC Complement. Med. Ther.* **2024**, *24*, 264, doi:10.1186/s12906-024-04578-z.
187. Pyun, H.; Kang, U.; Seo, E.K.; Lee, K. Dehydrocostus lactone, a sesquiterpene from Saussurea lappa Clarke, suppresses allergic airway inflammation by binding to dimerized translationally controlled tumor protein. *Phytomedicine* **2018**, *43*, doi:10.1016/j.phymed.2018.03.045.
188. Wang, M.R.; Huang, L.F.; Guo, C.; Yang, J.; Dong, S.; Tang, J.J.; Gao, J.M. Identification of NLRP3 as a covalent target of 1,6-O,O-diacetylbritannilactone against neuroinflammation by quantitative thiol reactivity profiling (QTRP). *Bioorg. Chem.* **2022**, *119*, doi:10.1016/j.bioorg.2021.105536.
189. Zhang, H.H.; Kuang, S.; Wang, Y.; Sun, X.X.; Gu, Y.; Hu, L.H.; Yu, Q. Bigelovin inhibits STAT3 signaling by inactivating JAK2 and induces apoptosis in human cancer cells. *Acta Pharmacol. Sin.* **2015**, *36*, doi:10.1038/aps.2014.143.
190. Khan, M.; Maryam, A.; Saleem, M.Z.; Shakir, H.A.; Qazi, J.I.; Li, Y.; Ma, T. Brevilin A induces ROS-dependent apoptosis and suppresses STAT3 activation by direct binding in human lung cancer cells. *J. Cancer* **2020**, *11*, doi:10.7150/jca.40983.
191. Liu, L.; Chen, X.; Jiang, Y.; Yuan, Y.; Yang, L.; Hu, Q.; Tang, J.; Meng, X.; Xie, C.; Shen, X. Brevilin A Ameliorates Acute Lung Injury and Inflammation Through Inhibition of NF-κB Signaling via Targeting IKKα/β. *Front. Pharmacol.* **2022**, *13*, doi:10.3389/fphar.2022.911157.
192. Lu, Q.; Zhu, J.; Teng, L.; Chen, C.; Bi, L.; Chen, W. Britannin inhibits hepatocellular carcinoma development and metastasis through the GSK-3β/β-catenin signaling pathway. *Phytomedicine* **2024**, *135*, 156126, doi:10.1016/j.phymed.2024.156126.
193. Büchele, B.; Zugmaier, W.; Lunov, O.; Syrovets, T.; Merfort, I.; Simmet, T. Surface plasmon resonance analysis of nuclear factor-κB protein interactions with the sesquiterpene lactone helenalin. *Anal. Biochem.* **2010**, *401*, doi:10.1016/j.ab.2010.02.020.
194. Chen, H.; Hu, Q.; Wen, T.; Luo, L.; Liu, L.; Wang, L.; Shen, X. Arteannuin B, a sesquiterpene lactone from Artemisia annua, attenuates inflammatory response by inhibiting the ubiquitin-conjugating enzyme UBE2D3-mediated NF-κB activation. *Phytomedicine* **2024**, *124*, doi:10.1016/j.phymed.2023.155263.
195. Tang, P.; Zhao, S.; Wang, X.; Wang, S.; Wang, Y.; Kong, L.; Luo, J. Chloranthalactone B covalently binds to the NACHT domain of NLRP3 to attenuate NLRP3-driven inflammation. *Biochem. Pharmacol.* **2024**, *226*, 116360, doi:10.1016/j.bcp.2024.116360.
196. Chen, J.J.; Yan, Q.L.; Bai, M.; Liu, Q.; Song, S.J.; Yao, G.D. Deoxyelephantopin, a germacrane-type sesquiterpene lactone from Elephantopus scaber, induces mitochondrial apoptosis of hepatocarcinoma cells by targeting Hsp90α in vitro and in vivo. *Phyther. Res.* **2023**, *37*, doi:10.1002/ptr.7654.
197. Lagoutte, R.; Serba, C.; Abegg, D.; Hoch, D.G.; Adibekian, A.; Winssinger, N. Divergent synthesis and identification of the cellular targets of deoxyelephantopins. *Nat. Commun.* **2016**, *7*, doi:10.1038/ncomms12470.
198. Hong, L.; Chen, J.; Wu, F.; Wu, F.; Shen, X.; Zheng, P.; Shao, R.; Lu, K.; Liu, Z.; Chen, D.; et al. Isodeoxyelephantopin Inactivates Thioredoxin Reductase 1 and Activates ROS-Mediated JNK Signaling Pathway to Exacerbate Cisplatin Effectiveness in Human Colon Cancer Cells. *Front. Cell Dev. Biol.* **2020**, *8*, doi:10.3389/fcell.2020.580517.
199. Ferraro, G.; Voli, A.; Mozzicafreddo, M.; Pollastro, F.; Tosco, A.; Monti, M.C. Targeting phosphoglycerate kinases by tatridin A, a natural sesquiterpenoid endowed with anti-cancer activity, using a proteomic platform. *Front. Mol. Biosci.* **2023**, *10*, doi:10.3389/fmolb.2023.1212541.
200. Chin, C.-H.; Chen, S.-H.; Wu, H.-H.; Ho, C.-W.; Ko, M.-T.; Lin, C.-Y. cytoHubba: identifying hub objects and sub-networks from complex interactome. *BMC Syst. Biol.* **2014**, *8*, S11, doi:10.1186/1752-0509-8-S4-S11.
201. Kim, J.; Patel, M.; Ruzevick, J.; Jackson, C.; Lim, M. STAT3 Activation in Glioblastoma: Biochemical and Therapeutic Implications. *Cancers (Basel).* **2014**, *6*, 376–395, doi:10.3390/cancers6010376.
202. Takaesu, G.; Ninomiya-Tsuji, J.; Kishida, S.; Li, X.; Stark, G.R.; Matsumoto, K. Interleukin-1 (IL-1) receptor-associated kinase leads to activation of TAK1 by inducing TAB2 translocation in the IL-1 signaling pathway. *Mol. Cell. Biol.* **2001**, *21*, 2475–2484, doi:10.1128/MCB.21.7.2475-2484.2001.
203. He, Y.; Hara, H.; Núñez, G. Mechanism and Regulation of NLRP3 Inflammasome Activation. *Trends Biochem. Sci.* **2016**, *41*, 1012–1021, doi:10.1016/j.tibs.2016.09.002.